NRDL TD-146

410924

Copy No. 27

SPECTROMETRIC ANALYSIS OF GAMMA RADIATION FROM FALLOUT FROM OPERATION REDWING

Research and Development Technical Report USNRDL-TR-146

29 April 1957

by

W. E. Thompson

Statement A
Approved for public release;
Distribution unlimited.

U.S. NAVAL RADIOLOGICAL DEFENSE LABORATORY
SAN FRANCISCO 24 · CALIFORNIA

[redacted]

SUMMARY

Gamma radiation emitted by selected fallout samples collected at Operation REDWING was spectrometrically analyzed for the purpose of determining its characteristics (expressed in terms of absolute photon intensities for each discernible gamma line) as a function of time after shot.

Since the absolute photon intensities are given and most samples represent known fractions of the area of the fallout collectors, one result is that dose rates in the vicinity of the collecting site can be calculated.

Another important result of the analysis suggests that Na^{24} becomes an increasingly important contributor to the radiation hazard from fallout at early times after detonation [redacted]

[redacted]

[redacted]

ADMINISTRATIVE INFORMATION

This report is one of a series of technical reports on the gamma-ray spectra of fallout samples collected at various weapon tests. Previous data has been reported in this laboratory's USNRDL-420, 31 August 1953, USNRDL-TR-32, 26 January 1955, and USNRDL-TR-106, 27 August 1956. The sample study reported here was conducted in conjunction with Project 2.6.3, Operation REDWING.

The work was done under Bureau of Ships Project No. NS 081-001, Technical Objective AW-7, and is a continuation of that described as Subtask 6 in this laboratory's report to the Bureau of Ships, DD Form 613, July 1956. Similar work is described under Program 9, Problem 1, in this laboratory's Semi-annual Progress Report, 1 July to 31 December 1956, Progress Report USNRDL-P-1, January 1957.

[redacted]

[redacted]

ACKNOWLEDGMENTS

The author wishes to acknowledge the assistance of Dr. R. L. Mather and Dr. C. S. Cook whose suggestions and critical review of the report were greatly appreciated.

The assistance of Dr. D. L. Love and Mr. J. L. Mackin of Analytical and Standards Branch of Chemical Technology Division in preparing the calibrated standards is gratefully acknowledged.

The excellent liaison both in regard to samples and information between Radiological Capabilities Branch of Chemical Technology Division and this Section was provided by Mr. W. Williamson, Jr.

The Gaussian curve generator was constructed by Mr. P. S. Applebaum.

Members of the Electronics Section were cooperative at all times.

[redacted]

[redacted]

INTRODUCTION

Analyses have been made at USNRDL with a single-channel gamma-ray spectrometer of radiation emitted by 21 selected radioactive fallout samples collected by Project 2.6.3 at the Spring, 1956, weapons test series known as Operation REDWING at the Pacific Proving Grounds. These measurements were made to determine the spectrometric characteristics of the fallout radiation versus time and to compare these characteristics for consistency among samples from the same and different shots.

The present work is a continuation of the spectrometric analyses of fallout gamma radiation which have been made at Operation UPSHOT-KNOTHOLE at the Nevada Test Site in 1953[1], Operation CASTLE at the Pacific Proving Grounds in 1954[2], and Operation TEAPOT at the Nevada Test Site in 1955 [3,4], taking advantage of further refinements in instrumentation and analyzing technique.

Project 2.6.3 collected samples of various types at several ship, barge and land stations and returned them to NRDL by air. This rapid return allowed analysis to begin as early as 51 hours after shot time--a notable improvement over the earliest-time receipt of 4 days accomplished at Operation CASTLE. Other samples requiring specialized handling, i.e. weighing, aliquoting, evaporation,

[redacted]

[redacted]

etc., reached the investigator at various times, some as late as ten days after shot time.

The results show absolute photon source strengths for each energy from the various samples, while in previous reports only relative line intensities were given. Since each sample constituted an accurately determined portion of the material taken from a fallout collector of known area, an estimate can be made concerning the total gamma source strength per unit area in the vicinity of the collecting site.

Other than reporting quantitative information on photons emitted per square inch of fallout collection area, this experiment exemplified better organization and preparation in other ways. The samples were prepared in standardized containers so that changing geometry was never a problem. The spectrometer was "well-seasoned" and dependable and was used without modification throughout the course of the experiment. The instrument was improved by the substitution of a Moseley X-Y plotter for the Brown recorder. Finally the analysis itself was made simpler and more consistent by the use of a better way of measuring peak areas.

[redacted]

[redacted]

INSTRUMENTATION

A gamma-ray photon is detectable only by means of the energy it loses in an interaction or interactions with matter. Gamma-ray photons lose energy by three main processes: photoelectric effect, Compton effect, and positron-negatron pair production. The cross-section for each effect is dependent on the energy of the gamma-ray photon and the atomic number of the detecting material.

The energy given up by the gamma-ray photon undergoing any of these processes ultimately manifests itself in the molecular excitation of the detecting material. Many organic crystals(such as anthracene, stilbene, and diphenylbutadiene)and many inorganic crystals(such as thallium-activated sodium iodide, indium- or thallium-activated lithium iodide, and potassium iodide) relieve this excitation in the form of useful scintillations of light whose predominant color depends on the crystal.

The intensity of the light flashes produced in these materials is dependent (in some cases, linearly) on the energy of the incident photon (provided it is totally absorbed). These light pulses are detected by a photomultiplier tube which converts them into electrical pulses.

[redacted]

These pulses are amplified then analyzed according to peak voltage and counted.

NaI(Tl) crystals are in wide use today as gamma-ray detectors because of their high efficiency and linearity. The disadvantage of their being hygroscopic is largely overcome by sealing them hermetically in thin-walled aluminum containers.

For this experiment a special sample holder was made for the spectrometer which allowed the bottoms of the sample containers to be placed 2 inches above the top of the collimator (a 1/2-inch hole through 6 inches of lead) and centered without further adjustment.

The 4-inch in diameter by 4-inch long NaI(Tl) crystal, 5-inch Du Mont photomultiplier tube, preamplifier and housing (Fig. 1) were the same as those used in the analysis of the data from Operation TEAPOT[3] and are more fully described elsewhere.[4]

The output of the preamplifier was fed into a Tracerlab non-overloading linear amplifier whose output pulses were analyzed by an Atomic Instrument Company Model 510 pulse height analyzer, the variable base line bias of which was provided by a helipot, motor driven through its range.[5] The output pulses from the analyzer were fed into

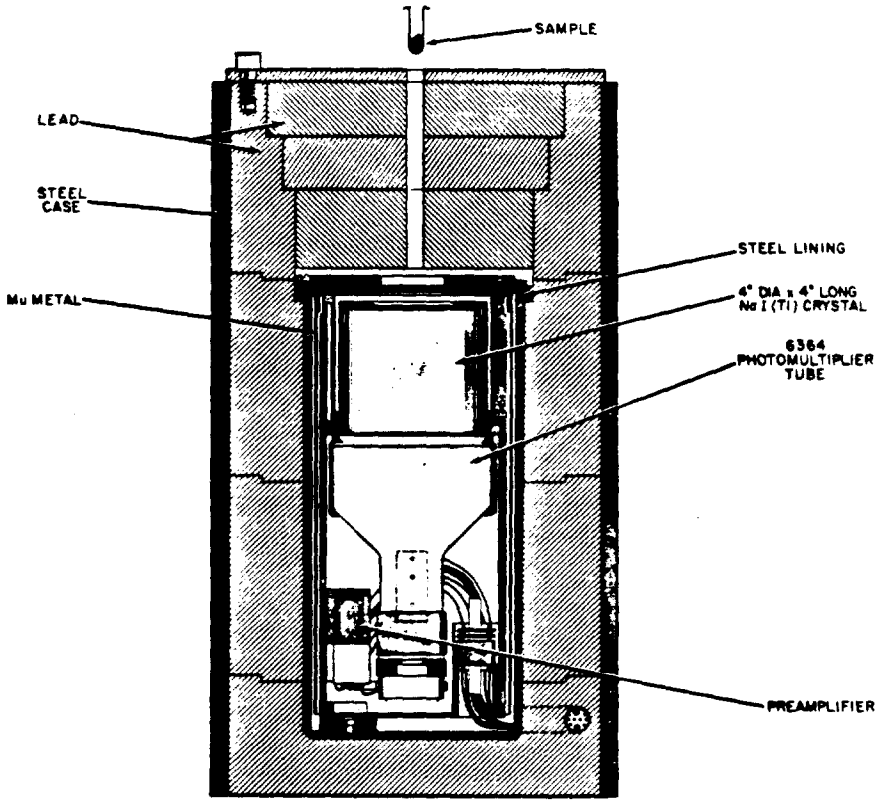

Fig. 1 Crystal, Photomultiplier Tube and Housing.[3] The lead shield is 2½ in. thick on the sides and bottom and 6 in. thick on top with a ½-in. hole directed toward the crystal face to provide collimation.

[redacted]

an NRDL-designed[4] count-rate meter. This count-rate meter has 7 scales ranging in sensitivity from 10 counts per second full scale to 1000 counts per second full scale. The output of the count-rate meter controlled the Y coordinate of a Moseley Autograf X-Y plotter, while the X coordinate was varied by the base line bias of the analyzer. A modification in the form of a potentiometer in series with the X input allowed fine adjustments to be made in matching pulse height to particular lines on the recording paper. A typical recording made by the X-Y recorder is shown in Fig. 2.

The regulated high-voltage supply for the photomultiplier tube was constructed from a UCRL design.

PROCEDURE

The fallout samples were supplied by Project 2.6.3 in 3/4-inch in diameter by 2-inch in length polystyrene containers each containing approximately 50-1000 microcuries total activity. Descriptive information about each sample, the effective fallout area it represents, and its associated shot is listed in Table I*.

Samples were obtained from 2 types of collectors. The cloud sample consisted of material caught on a filter paper through which a representative sample of air was drawn as an aircraft flew through the cloud following the detonation.

* The tables appear at the end of the text.

[redacted]

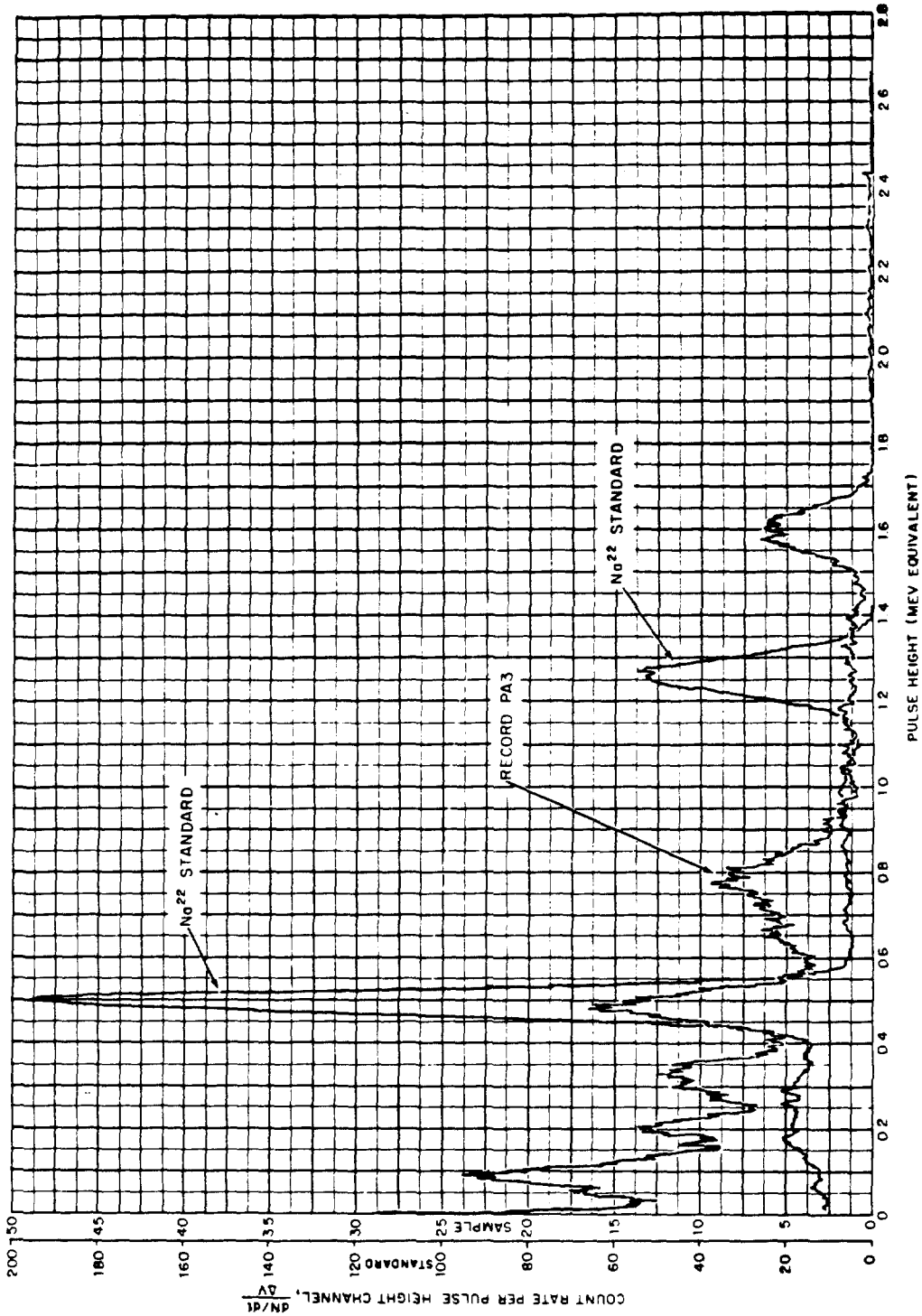

Fig. 2 Typical Spectrum. Record, PA3 on 50 C/S Scale, Standard was Recorded on 200 C/S Scale.

[redacted]

The open-close total collector (OCC)[6,7] was designed to collect and hold fallout material while reducing to a minimum the amount of extraneous material deposited both before and after the collecting period. When triggered either by an increase in radioactive background or by hand, the cover of the device opens and a collecting tray rises into the wind stream for the preset exposure time (variable in 15-minute increments between 0 and 81 hours). The tray has an effective collecting area of about 2.5 square feet divided into numerous cells to reduce loss of material due to wind. Samples, other than cloud samples, were obtained from this type of collector mounted on converted liberty ships (YAG's), barges (YFNB's) and How Island.

After collection the fallout material was flown back to the Laboratory and aliquoted by Chemical Technology Division. The aliquots supplied to this section for analysis were placed in the polystyrene containers and prevented from shifting, in the case of granular or pulverized samples, by the addition of a small amount of paraffin.

The machine was calibrated so that on "standard" gain the total absorption peak of a 100, 200, or 300, etc., kev gamma ray would be centered on the 1/2-inch, 1-inch, or 1-1/2-inch, etc., line on the recording paper. This calibration was accomplished first by careful zero-setting of the X-Y

[redacted]

[redacted]

recorder and analyzer, and then by varying the gain of the amplifier and the fine pulse-height adjustment on the recorder until total absorption peaks from standards of known gamma energies (Hg^{203}, Na^{22}, and Cs^{137}) fell at the appropriate positions on the recording paper (Fig. 2). It was found that this calibration was very stable, requiring only an occasional small adjustment in the zero-set control of the recorder to allow for variation in paper placement and ruling defects on the paper. That the equipment was essentially stable in the Y direction was shown by periodic checks with the 60-cycle test position of the count-rate meter and by the linearity of the decay curves on semi-logarithmic paper of the calibrated standards.

Pulse height spectra were recorded for each sample on standard gain (3 Mev full scale) and on "high" gain--amplifier gain increased by a factor of four (0.75 Mev full scale)--in those cases where the strength of the sample allowed it. How long the taking of periodic recordings of each sample could continue after shot time before the count rate became too low for statistically significant results depended of course, on the original strength of the sample.

On nearly all of the standard-gain records, a calibrated Na^{22} standard source was recorded on the same sheet in a different color ink, while on the high-gain records a

[redacted]

[redacted]

calibrated Hg^{203} source was used. This use of the calibrated standards allowed a constant check to be made on the stability of the equipment (see Appendix I).

ANALYSIS OF DATA

The pulse height spectrum of a monoenergetic gamma ray consists of a total absorption peak and continuous "Compton" distribution. If the energy of the gamma ray is above 1.02 Mev, pair production begins to take place and one of two secondary peaks is contributed to, according to whether one or both of the annihilation quanta escape from the crystal. The peaks all have the shape of normal distribution functions or "Gaussians" because of the statistical nature of the photoelectric effect and the secondary-emission phenomenon inherent in the operation of a photomultiplier tube.

If two incident gamma energies are present, the lower is superimposed additively on the continuous Compton distribution of the higher. An example of the idealized addition of three different monoenergetic gamma rays is shown in Fig. 3. As more gamma energies are added the resulting confusion becomes progressively worse. (If the higher energies are above 1.02 Mev, the presence of annihilation radiation escape peaks further complicates the spectrum and thus the analysis.)

[redacted]

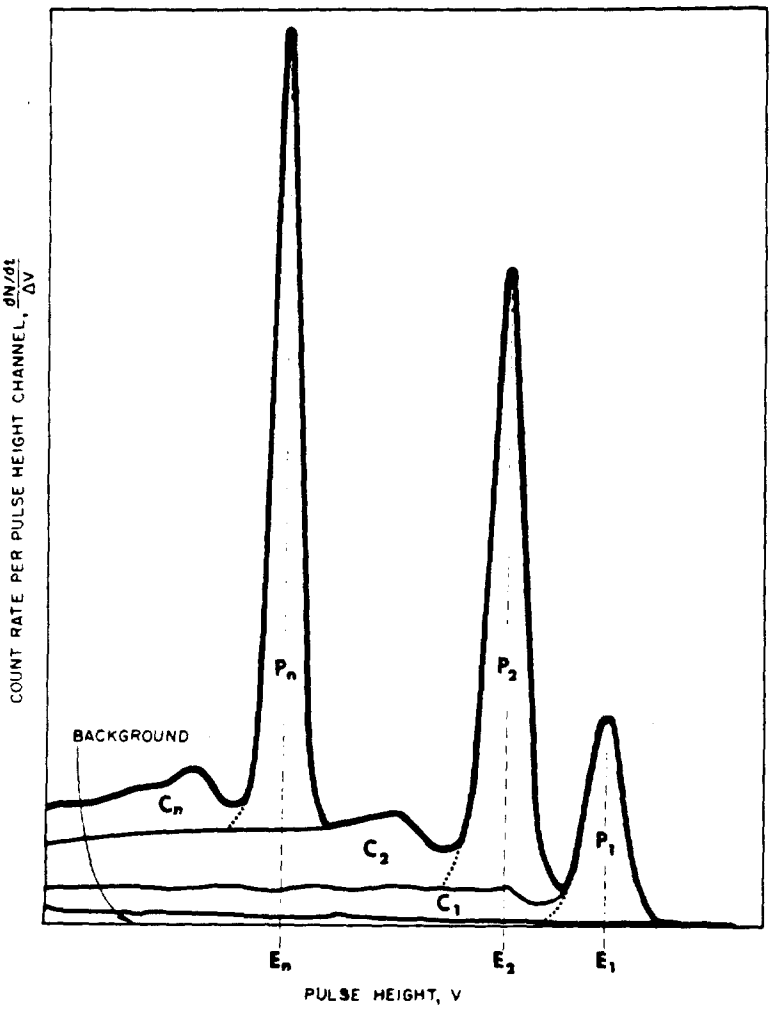

Fig. 3 Addition of Three Total Absorption Peaks at Different Energies and Their Associated Compton Distributions Showing the Resultant Spectrum (heavy line).[3]

In order to untangle these overlapping distributions and arrive at the basic gamma lines, a method of graphical unfolding is used. One starts at the highest-energy peak present (assuming that it is not superimposed on the Compton distribution of a still higher energy) and measures the area under the total absorption peak. Then knowing the peak-to-total ratio (the method of ascertaining this ratio is described later) for each energy, one can calculate the area of the Compton distribution. After drawing in the Compton distribution of the highest energy, the process is repeated for the next highest-energy peak using the Compton of the highest energy as a base line. The process is continued until all the energies present are analyzed. Knowing the resolution of the instrument for each energy, one can tell whether there is only one energy contributing to a particular peak, or two or more unresolved energies present, by the width of the peak. The resolution (width of a peak in kev at half-maximum height) was determined by measuring the resolution for several total absorption peaks of known energy and plotting the results (Fig. 4).

In order to facilitate the measuring of the photopeak areas and to aid in estimating the relative size of two unresolved peaks, a series of Gaussian curves of predetermined widths, various heights and, thus, known areas, were drawn by means of a Gaussian curve generator (see Appendix II). By

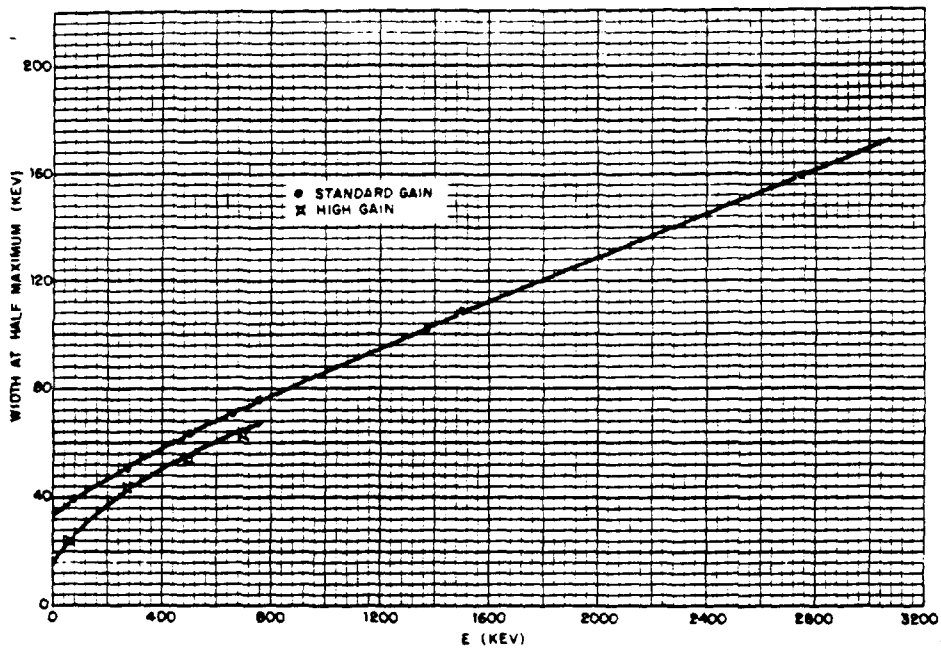

Fig. 4 Instrument Resolution Versus Gamma Energy

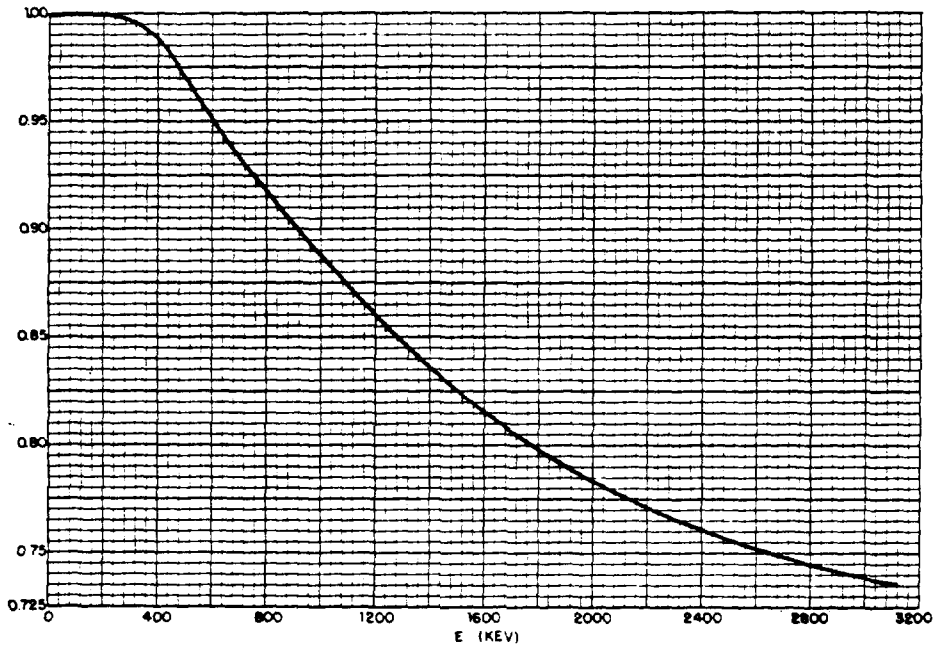

Fig. 5 Crystal Interaction Probability, v, Versus Gamma Energy, E.

[redacted]

superimposition of the suitable Gaussian on the pulse height spectrum with the aid of a frosted-glass light table, the area of each total absorption peak was determined without tedious measuring with a planimeter. For errors incurred by this measuring system see the section on errors.

The ratio of absolute photon intensity to total absorption peak area is some function of the energy of the gamma ray, $I/A = f(E)$. For the determination of the graphical relationship between I/A and E, it was first necessary to ascertain further machine parameters and other energy-dependent factors. These were:

(1) Crystal interaction probability, v. This is simply the fraction of incident photons of a particular energy which interacts in the crystal and is given by:

$$v = 1 - \exp(-\mu_x X)$$

where μ_x is the total linear absorption coefficient for gamma rays in sodium iodide[8] and X is the crystal length. For a crystal 10.16 cm (4 inches) in length, v versus E is shown plotted in Fig. 5.

(2) Peak-to-total ratio, w. This factor is determined experimentally by recording the spectra of several sources of known gamma energy and measuring areas of the total absorption peaks and the areas under the total spectrum. The ratios of these areas plotted against energy

[redacted]

[redacted]

furnish a fairly smooth curve. The peak-to-total curve characteristic of the machine used in the present experiment is shown in Fig. 6.

(3) Counts per second per square inch in the total absorption peak, C. This number is a constant of the machine and is found by dividing the number of counts per second per inch of deflection in the Y direction by the channel width in chart inches. The channel width used throughout the experiment corresponds to 0.1 inch on the chart paper and the total Y deflection is 10 inches. Then for the 200 c/s scale, C is 200.

(4) Source reduction factor, $\bar{K}$. This factor is the fraction of photons leaving the source which enter the crystal and takes into account effects of collimator penetration, finite extension of source, and solid angle subtended by the crystal from the source, assuming a point source and an opaque collimator. These effects are discussed in some detail in a theoretical paper by R. L. Mather of this laboratory.[9] Derived from information contained in this paper is Fig. 7, showing K, the source reduction factor for a point source, versus r, the distance of the source from the collimator axis. To find the average source reduction factor, $\bar{K}$, to account

[redacted]

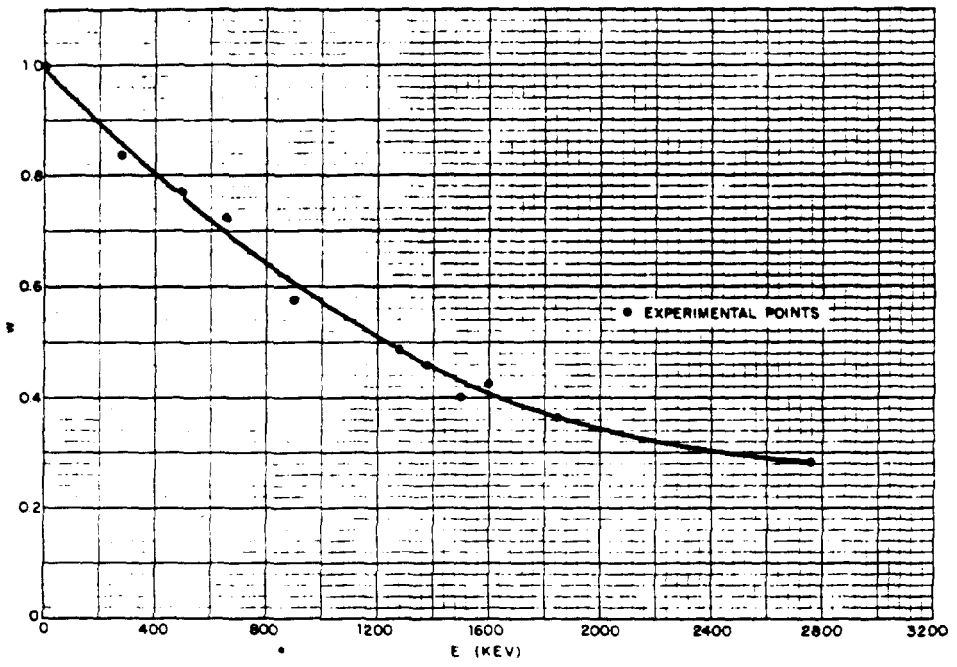

Fig. 6 Ratio, w, of the Area Under the Total Absorption Peak to the Area Under the Entire Pulse-Height Distribution Versus Gamma Energy

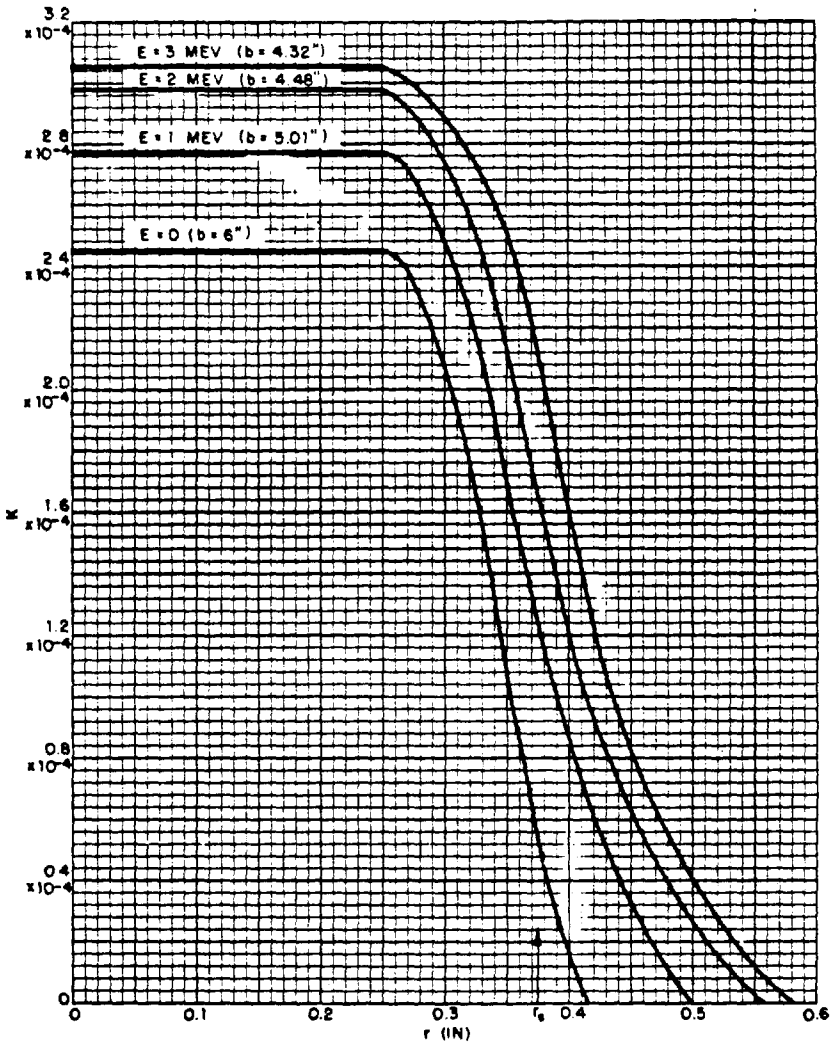

Fig. 7 Fraction, K, of Source Photons Entering Detector Versus Off-Axis Distance of Point Source for z = 5 in., a = $\frac{1}{2}$ in.

[redacted]

for the finite extension of the source, it was necessary to perform the following numerical integration:

$$\bar{K} = \frac{\int_0^{r_s} K r dr}{\int_0^{r_s} r dr}$$

where r_s is the radius of the extended source. The determination of $\bar{K}$ is somewhat simplified by the fact that K is constant over part of the range of r, i.e.:

$$K = a^2/16(z = b/2)^2 \quad (0 \leq r \leq a/2)$$

where a is the collimator diameter, b the collimator thickness and z the distance from the center of the collimator to the source. When r is larger than a/2 and smaller than az/b, K is some function of r determined graphically by interpolation and derived from Fig. 9 of Mather's paper. For values of r equal to or larger than az/b, K vanishes.

To make the reduction factor, $\bar{K}$, energy dependent, i.e., to include penetration effects, an approximation[9] is used. Penetration is a function of gamma-ray energy and the increased aperture due to increased energy is approximately the same as the geometrical aperture of an opaque collimator two mean-free-paths less thick.

For the particular geometry involved in the present experiment, the values of the machine parameters are as follows:

[redacted]

[redacted]

$a = 1/2$ inch

$z = 5$ inches

$r_s = 3/8$ inch

$b = (6 - 2/\mu)$ inches

where $1/\mu$ is the mean-free-path of gamma radiation in lead.

$\overline{K}$ was evaluated by means of numerical integration for values of E (and corresponding values of b) at 200-kev intervals between 0 and 2 Mev and at 3 Mev (Fig. 8).

The absolute photon intensity is a combination of these various correction factors, i.e.:

$$I = AC/vw\overline{K}$$

A graph of I/A versus E is shown in Fig. 9. After reading the energetically appropriate I/A from the graph, the number was multiplied by the area of the total absorption peak of the corresponding gamma ray to obtain absolute photon intensity of that line.

RESULTS

The absolute photon intensities with their estimated errors are listed for each gamma line of each record in Tables 2 and 3. The abbreviated sample notation used for

[redacted]

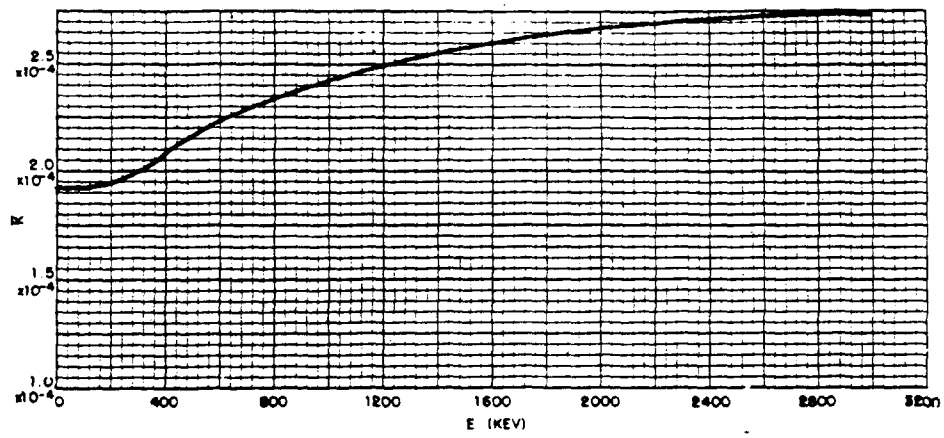

Fig. 8 Average Fraction, $\bar{K}$, of Source Photons Entering Detector (including collimator penetration) Versus Gamma Energy

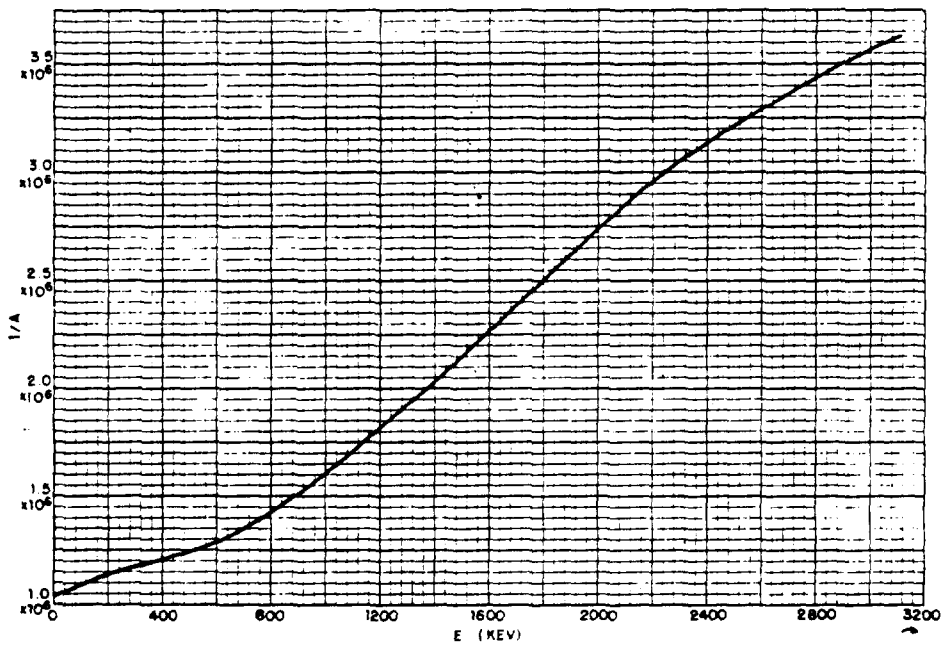

Fig. 9 Ratio, I/A, of Photons per Second From Source to Area Under Total Absorption Peak (in in.^{2}) for the 200 C/S Scale Versus Gamma Energy

brevity in Tables 2 and 3 is explained in Table 1. Table II contains the information obtained from the standard gain recordings and Table 3 lists the photon intensities found from the high gain (4×) recordings. Because of the increase in resolving power some lines which were unanalyzable or undetectable on the standard gain records became analyzable on the high gain records.

The data have been left in tabular form to make the information more readily accessible to those who wish to use it.

ERRORS

In actual practice the analysis is more difficult than might be assumed from the description in the Analysis of Data section for the following reasons:

(1) The shape of the Compton distribution is known only approximately for a given energy even though its area is known fairly accurately. Even if the shape were accurately known, it would be mechanically difficult to draw such a distribution in with a predetermined area. For this reason a straight line is used for the Compton distribution, with the resulting rectangle having the proper area. It is found, however, after drawing in this rectangular representation of the Compton distribution several times and getting the "feel" of the machine, that the base line for each succeeding peak can be estimated with similar accuracy

and considerably greater speed. Either way, of course, this approximation contributes to the overall error, the errors becoming progressively greater toward the lower energies.

(2) If two or more energies are present too close together to be resolved, one can draw two or more Gaussians of the proper width beneath the broad peak representing these unresolved energies, but it is difficult if not impossible to determine which of the energies is preponderant. In this case one can do little more than estimate. The energies present in this way therefore have larger estimated errors associated with them.

(3) Because of statistical fluctuations due to the low count rate on many samples, the curves drawn by the X-Y recorder are not smooth and the size of the peaks is somewhat questionable. On records where low count rate exists, therefore, the associated errors are estimated to be larger.

For comparison between areas determined by superimposition of generated curves and areas measured with the planimeter, several total absorption peaks were measured by both methods. The disparity between those peaks so compared ranged from 0 to 3 percent. This error is in general less than the statistical error.

found by taking the square root of the total number of counts contained in a rectangular area whose width is determined by the width of the Gaussian at the point where it ceases to coincide with the machine-drawn peak. This area is presumed to be the actual area compared. The statistical error found in this way varies widely (because of the great range in count rate), but for the peaks tested it varies between 2 and 6 percent.

A hindrance to accurate superimposition of the Gaussian curves on the total absorption peaks, contributing further to the error, may be the slight non-Gaussian character of the total absorption peak caused by the lack of perfect homogeneity of the crystal's light production.

To get some idea of how much of each spectrum occurred in analyzable peaks, the total areas of several spectra were measured with the planimeter and compared with the sums of the total areas associated with each listed energy (found by dividing each peak area by the appropriate peak-to-total ratio). It was found by this method that from 70 to 90 percent of a spectrum was accounted for in the peak-by-peak analysis.

The errors associated with the photon intensities shown in Table 2 are the result of estimates of the cumulative errors discussed above. They range from 3 percent for peaks with good resolution, good count rate, and good fit with the

[redacted]

superimposed Gaussian curves to 50 percent for peaks poor in all respects. Occasionally there is present an energy which is too small in photon intensity even for a good estimate to be made as to the quantity. The symbol ≥ 0 is used in the appropriate column in Table 2 to indicate the presence of such an energy. More rarely the symbol $\underline{>>0}$ is used to indicate the presence of an energy too poorly resolved (although not necessarily very small in intensity) to warrant an estimated quantitative listing.

In some cases there appear to be discrepancies between photon intensities from the same lines taken at nearly the same time for the two gain settings. Most of these intensities are not discrepant, however, by much more than the estimated error would allow. In those cases where the difference is too large, the estimated errors should be increased.

However, some of the differences seem predominantly one-sided. This inconsistency is especially noticeable for some of the 220 kev lines, i.e., areas recorded at high gain are lower than comparable areas recorded at standard gain, sometimes by as much as 30 percent. This effect appears in the resolution curves of Fig. 4. For many of the 105 kev lines compared, the effect is reversed, i.e. the areas recorded at high gain are higher than comparable areas recorded at standard gain. It is possible to account for the latter

[redacted]

[redacted]

effect by considering the greater effect an integrating time constant, such as is used in the count rate meter, has on low pulse heights.[10] No mechanism to explain the former effect suggests itself, however, and the fact that fair agreement exists in most cases between comparable 60-kev and 280-kev lines leads one to doubt the existence of a consistent energy-dependent machine effect to explain the discrepancies.

It may be that the disagreements are largely due to resolution problems in the low energy region of the standard gain records, since in many cases the areas could be brought closer to agreement by taking from one line and adding to an adjacent line. This problem is especially troublesome in trying to separate the 60, 105, and 140 kev lines on the standard gain records.

A discussion of the overall performance of the system in analyzing the standard sources, including the consistency of the results, is found in Appendix I.

DISCUSSION

It is of special interest to note the presence of Na^{24} activity in both the Zuni and Navaho cloud samples (the only samples to reach this section soon enough for such detection were the cloud samples from each shot). This activity is evident from the 1.37- and 2.75-Mev total absorption peaks detectable on the first two or three recordings made with each of these samples. [redacted]

[redacted]

[redacted]

If a fission-product decay curve of $t^{-1.2}$ and a 15-hour half-life for Na^{24} are assumed, then the maximum ratio of Na^{24} activity occurs 26 hours after shot time. The intensities of the 2.75 Mev and 1.37 Mev lines may be extrapoleted back to this time to give a maximum percentage Na^{24} contribution. [redacted]

[redacted]

[redacted]

Na^{24} is a major source of radiation hazard in fallout radiation one day past shot time.

There are several possible mechanisms for the production of Na^{24} by neutron induction: $Al^{27}(n,\alpha)Na^{24}$, $Mg(n,p)Na^{24}$, and $Na^{23}(n,\gamma)Na^{24}$ with respective cross sections of about 100 mb for 14-Mev neutrons, 191 ± 35 mb for 14.5-Mev neutrons and about 0.5 b for thermal neutrons.[11] [redacted] However, at the time of writing enough detailed information was not immediately available to permit intelligent speculation on which of these processes predominates.

Another interesting result apparent on most of the series of recordings begun at early enough times is the build-up of the 1.59-Mev activity from La^{140}. The fact that there is evidence of an increase in this activity at early times indicates that most of the original fission product of the mass number-140 series was Ba^{140} or a percursor. Assuming that all of the Ba^{140}-La^{140} fission-product complex was Ba^{140} originally, the build-up of the 1.59-Mev activity should reach its maximum at 136 hours after shot time. Theoretically there should be no build-up in

[redacted]

activity if the original contribution of La^{140} to this parent-daughter complex is more than 11.5 percent of the total activity of the combination. The evidence in the records of samples whose analysis was begun early enough for the build-up to show up, points toward their being very little or no La^{140} produced as an instantaneous fission product. This conclusion is borne out by studies of fission product yields from U^{235} made by Yaffe, et al.,[12] and Petruska et al.[13], who report yields of 6.32 ± 0.24 percent of Ba^{140} and 6.33 ± 0.32 percent of Ce^{140}, respectively. Since the difference is zero within experimental error, La^{140} is not produced as an original fission product.

The samples collected at ground and ship stations may be different due to fallout fractionation and possible anisotropies in fission-product ejection from the weapons.[3] That there is evidence that one or both of these mechanisms are operating can be ascertained by comparison of the spectra of samples collected at different places for the same shot. No pattern is discernible however, with so few sample collection locations. Therefore it is not possible to say anything more than that there seem to be discrepancies between samples from the same shot which are too large to explain in terms of measurement error alone, e.g., the 330-

[redacted]

kev activities present in records QA2 and RA2 (see Table 1 for notational definitions) differ by more than a factor of 3 in percentagewise contribution. Also the 105-kev activities in BA7 and GA2 differ by more than a factor of 3.

Dose rates measured 3 feet above the surface of How Island in the vicinity of the collecting sites have been plotted as a function of time after burst[14] for Shot Zuni. The dose rates calculated from the photon intensities, listed in Table 2, of the two samples received from the How Island collection stations (GA and IA), when compared for the proper times with the curve drawn from the measured dose rates, agree within experimental error.

Approved by:

A. Guthrie

A. GUTHRIE
Head, Nucleonics Division

For the Scientific Director

[redacted]

[redacted]

APPENDIX I STANDARDS CALIBRATION

Calibrated standard sources were supplied to this group by Analytical and Standards Branch of Chemical Technology Division to allow checks to be made of the relationship between area of total absorption peaks and their associated photon intensities, and to provide standards of known energy for record by record energy calibration. The calibrated standards used were 75.6 (±4 percent) microcuries of Na^{22} and 145 (±5 percent) microcuries of Hg^{203}. The standards were calibrated on May 18, 1956.

In order to use these standards to check the correctness of the I/A versus E curves, corrections had to be made in the source strengths listed. In the case of Na^{22} the standards were calibrated in terms of positron emission alone, so that to arrive at the 1.28 Mev photon intensity, account had to be taken of the 6 to 11 percent electron capture.[15,16] When this correction is applied, the original 1.28 Mev photon source strength becomes 80.4 to 84.9 "microcuries" or 2.97×10^6 to 3.14×10^6 photons per second. To compare this number to that obtained by multiplying the area of the total absorption peak by I/A for 1.28 Mev, the area must first be found by extrapolating the decay curve back through the calibration date. This area is 1.54 (±2

[redacted]

[redacted]

percent) square inches and gives 2.90×10^6 when multiplied by the proper I/A from Fig. 9. The latter intensity is from 2.5 to 7.6 percent lower than the intensity determined from the calibration of the standard, but agrees within the experimental error.

The comparison of the Hg^{203} photon intensities proceeds similarly to the Na^{22} comparison. The Hg^{203} source strength was given in actual disintegrations per second but only 78.7 of these disintegrations result in 279-kev gamma rays because of the internal conversion in Hg^{203}. After the appropriate corrections are made the photon intensities obtained from the extrapolated total absorption peak area and calibrated source strength are 4.15×10^6 (±5 percent) and 4.22×10^6 (±5 percent) photons per second respectively. The intensities obtained by the two methods differ by less than 2 percent well within experimental error.

With 54 recordings of the 145 μc Hg^{203} standard and 94 recordings of the 75.6 μc Na^{22} standard made over a period of several months already available, it was decided to make a least squares fit of the decay curve to get a quantitative idea of the machine's stability. It was assumed that the functional form of the equations relating area to time was $A = \exp(-\lambda t)$ or a polynomial of the form $y = a_o + a_1 t$ (a straight line) where $y = \ln A$.

[redacted]

The coefficients a_1 were found by solution of the simultaneous equations:

$$s_o a_o + s_1 a_1 = m_o$$

$$s_1 a_o + s_2 a_1 = m_1$$

where $s_k = \sum_{n=1}^{N} t_n^k$, $m_k = \sum_{n=1}^{N} t_n^k y_n$, and N is the number of measured areas. The details are not shown here but the results are as follows:

For Hg^{203}: $y = 1.3022 - 0.0154t$.

For Na^{22}: $y = 0.4336 - 0.0014t$.

Areas were computed from the equations for each day that spectra were made and compared with the measured areas. The average deviation for Na^{22} was 0.03 in^2 and for Hg^{203} was 0.106 in^2. The average percentage deviation was 2.0 percent for Na^{22} and 5.4 percent for Hg^{203}. The probable reason for the higher deviation for Hg^{203} is a combination of fewer records, shorter half life (requiring progressively more sensitive count-rate scales with consequent loss in statistical accuracy during the latter part of the recording period) and higher amplifier gain requiring the use of more sensitive count-rate scales to provide peaks of adequate height.

APPENDIX II THE GAUSSIAN CURVE GENERATOR

The Gaussian curve generator consisted of a Gaussian template mounted on a lucite disk which in turn was mounted like a wheel on the shaft of a potentiometer. With a battery to provide voltage and another potentiometer to vary the amount of voltage across the main potentiometer, the pen of the X-Y recorder was caused to move along the X axis as the wheel was turned. The range of the pen's motion during one revolution of the wheel was governed by the setting of the secondary potentiometer. A photovoltaic cell "looking" at a light through the template was connected to the Y axis of the X-Y recorder with another potentiometer controlling its range. As the wheel was turned by hand and the amount of light reaching the cell was varied by the template, a Gaussian curve of height and width, as determined by the range-controlling potentiometers, was drawn on the recorder paper. The template was made of thin, opaque sheet metal and its shape was determined by plotting a Gaussian curve on polar graph paper.

By this method several hundred Gaussian curves were drawn of various heights for each width. The widths were chosen to correspond to the widths at half maximum for the actual energies present in the fallout spectra as determined from the resolution versus energy curve.

[redacted]

The areas in square inches of the Gaussian curves so drawn were determined by measuring their height and width (the same for each series of heights) and applying the formula (derived from the equation for a Gaussian curve):

$$A = 1.06 w_{\frac{1}{2}} n(0)$$

where $w_{\frac{1}{2}}$ is the width in inches at half maximum and n(0) is the maximum height in inches.

[redacted]

[redacted]

REFERENCES

1. Bouquet, F.L., Kreger, W.E., Mather, R.L., and Cook, C.S. Application of the Scintillation Spectrometer to Radioactive Fall-Out Spectra Analysis. (Operation UPSHOT-KNOTHOLE), U.S. Naval Radiological Defense Laboratory Report USNRDL-420, 31 August 1953 (CONFIDENTIAL).

2. Cook, C.S., Johnson, R.F., Mather, R.L., Tomnovec, F.M., and Webb, L.A. Gamma-Ray Spectral Measurements of Fall-out Samples from Operation CASTLE, U.S. Naval Radiological Defense Laboratory Technical Report USNRDL-TR-32 (AFSWP-822), 26 January 1955 (CONFIDENTIAL-RESTRICTED DATA).

3. Webb, L.A., Tomnovec, F.M., Mather, R.L., Johnson, R.F., and Cook, C.S. Analysis of Gamma Radiation from Fallout from Operation TEAPOT, U.S. Naval Radiological Defense Laboratory Technical Report USNRDL-TR-106, 27 August 1956 (CONFIDENTIAL-RESTRICTED DATA).

4. Mather, R.L., Taylor, R.A., et al. of this laboratory. Report in preparation on Operation TEAPOT instrumentation.

5. Ehat, R.F. Base Line Control and Sweep Monitor for Single Channel Pulse Analysis, U.S. Naval Radiological Defense Laboratory Technical Memorandum No. 55, 7 February 1956.

6. Appendix C to Operation Plan for Project 2.6.3, Operation REDWING, "Manual of Standard Instrumentation."

---

7. Triffet, T., LaRiviere, P.D., Evans, E.C., Perkins, W.W., and Baum, S. Characterization of Fallout. U.S. Naval Radiological Defense Laboratory, Project 2.6.3 Operation REDWING, Interim Test Report ITR-1317, February 1957 (SECRET-RESTRICTED DATA).

8. White, G.R. X-ray Attenuation Coefficients from 10 kev to 100 Mev. National Bureau of Standards Report NBS-1003, 13 May 1952.

[redacted] [redacted]

9. Mather, R. L. of this laboratory. Report in preparation on "Collimator Aperture with Penetration Effects."

10. Mather, R. L. of this laboratory. Unpublished data on "The Effect of an Integrating Time Constant on the Record of a Moving Channel Pulse Height Analyser."

11. Endt, P. M. and Kluyver, J. C. Rev. Mod. Phys. 26, No. 1:95 (1954).

12. Yaffe, L., Thode, H. G., Merritt, W. F., Hawkings, R. C., Brown, F. and Bartholomew, R. M. Can. J. Chem. 32:1017(1954).

13. Petruska, J. A., Thode, H. G., and Tomlinson, R. H. Can. J. Phys. 33:693 (1955).

14. Triffet, T., LaRiviere, P. D., Evans, E. C., Perkins, W. W., and Baum, S. Characterization of Fallout, Project 2.6.3, Operation REDWING, Final Report, WT-1317 in preparation, U. S. Naval Radiological Defense Laboratory.

15. Kreger, W. E. Phys. Rev. 96:1554 (1954).

16. Charpak, G. Journale de Physique et Le Radium 16:62 (1955).

[redacted]

TABLE I

Miscellaneous Sample Data

Site Designation	Sample Abbreviated Designation: Std Gain	Sample Abbreviated Designation: High Gain	Collector Type	Collector Location From GZ	Weight or Volume	Ground Area Representation ($in.^2$)
			Shot Cherokee, [redacted]			
Std Cloud	AA	AB	Filter Paper	Cloud	–	–
			Shot Zuni, [redacted]			
Std Cloud	BA	BB	Filter Paper	Cloud	–	–
YFNB "Whim" 1	FA	–	Deck[a]	10 mi ENE	–	–
How F-61	GA	GB	OCC[b]	13 mi ENE	10 ml	7.2
YAG 40 B-19	HA	HB	OCC	52 NNW	1.36 g	194.1
How F-67	IA	IB	OCC	13 mi ENE	0.57 g	62.5
YAG 40 B-6	JA	JB	OCC	52 mi NNW	10 ml	14.4
			Shot Flathead, [redacted]			
Std Cloud	KA	KB	Filter Paper	Cloud	–	–
YAG 39 C-36	LA	LB	OCC	29 mi NNE	–	–
YFNB-13-E-56	MA	MB	OCC	7.5 mi WNW	0.02 g	11.5
YFNB-13-E-54	NA	NB	OCC	7.5 mi WNW	10 ml	14.4
			Shot Navaho, [redacted]			
Std Cloud	OA	OB	Filter Paper	Cloud	–	–
YFNB-13-E-54	PA	PB	OCC	8.5 mi W	0.28 g	60.6
YFNB-13-E-56	RA	RB	OCC	8.5 mi W	10 ml	18.0
YAG 39 C-21	SA	–	OCC	21 mi NNW	10 ml	36.0
YAG 39 C-36	QA	QB	OCC	21 mi NNW	–	–
			Shot Tewa [redacted]			
Std Cloud	TA	TB	Filter Paper	Cloud	–	–
YAG 39 C-36	UA	UB	OCC	24 NNW	0.02 g	1.2
YFNB-13-E-56	VA	VB	OCC	10 mi SW	0.03 g	9.3
Y3-T-1C-D	WA	–	Seawater[c]	–	–	–
YFNB-13-E-54	XA	XB	OCC	10 mi SW	10 ml	14.4
YAG 39 C-21	YA	YB	OCC	24 mi NNW	10 ml	14.4

(a) Picked up at random from deck of YFNB-29.
(b) Open-close collector
(c) Evaporated sample from large open tank on deck.

[redacted]

[redacted]

TABLE 2

Absolute Photon Intensities (Standard Gain), in Millions of Photons Per Second Per Line for Each Sample

Time After Shot (hr)	Sample and Recording (a)	Line Designation (kev)(b) → 60	105	140	220	280	330	370	450	500	570	610	650	750	825	900
53	AA 1	0.73 ± 10(c)	3.32 ± 5	–	1.62 ± 4	1.16 ± 6	0.32 ± 10	–	0.20 ± 20	0.54 ± 10	0.20 ± 20	–	0.92 ± 10	0.88 ± 7	–	0.14 ± 20
74	2	0.60 ± 10	2.70 ± 5	–	1.37 ± 4	0.70 ± 20	0.37 ± 15	–	0.16 ± 20	0.37 ± 10	0.17 ± 20	–	0.77 ± 6	0.62 ± 10	0.14 ± 30	0.11 ± 20
98	3	0.46 ± 10	1.80 ± 5	–	0.88 ± 6	0.52 ± 10	0.26 ± 10	–	0.12 ± 20	0.30 ± 10	0.08 ± 25	–	0.46 ± 10	0.47 ± 12	–	0.08 ± 40
166	4	0.28 ± 10	1.13 ± 5	–	0.55 ± 6	0.29 ± 12	0.16 ± 12	–	–	0.26 ± 10	–	–	0.29 ± 10	0.28 ± 15	–	–
191	5	0.30 ± 10	0.72 ± 5	–	0.39 ± 10	0.23 ± 10	0.14 ± 15	–	0.09 ± 25	0.20 ± 12	–	–	0.21 ± 15	0.22 ± 15	–	–
215	6	0.24 ± 10	0.68 ± 10	–	0.38 ± 10	0.16 ± 10	0.11 ± 15	–	0.06 ± 20	0.20 ± 15	–	–	0.20 ± 15	0.18 ± 20	–	–
242	7	0.24 ± 15	0.58 ± 10	–	0.32 ± 10	0.12 ± 20	0.11 ± 20	–	0.07 ± 30	0.16 ± 20	–	–	0.13 ± 20	0.15 ± 20	–	–
262.5	8	0.19 ± 10	0.46 ± 10	–	0.22 ± 30	0.13 ± 25	0.10 ± 25	–	–	0.21 ± 15	–	–	0.10 ± 25	0.13 ± 20	–	–
335	9	0.15 ± 15	0.30 ± 10	–	0.18 ± 15	0.06 ± 25	0.07 ± 25	–	–	0.17 ± 20	–	–	0.05 ± 25	0.08 ± 40	–	–
405.5	10	0.10 ± 15	0.19 ± 10	–	0.14 ± 15	0.06 ± 30	0.06 ± 30	–	–	0.16 ± 25	–	–	0.06 ± 25	0.07 ± 50	–	–
597.5	11	0.05 ± 20	0.07 ± 15	–	0.04 ± 25	0.04 ± 50	0.03 ± 50	–	–	0.09 ± 30	–	–	0.03 ± 50	0.06 ± 40	–	–
53	BA 1	>>0	3.71 ± 5	>>0	2.62 ± 5	2.55 ± 7	0.76 ± 10	–	0.46 ± 20	3.32 ± 5	>>0	–	2.57 ± 5	2.05 ± 10	–	0.58 ± 20
69	2	1.20 ± 20	3.11 ± 5	0.83 ± 20	2.17 ± 3	2.04 ± 5	0.83 ± 10	–	0.44 ± 20	2.16 ± 8	>>0	–	1.99 ± 7	1.48 ± 7	–	0.38 ± 20
93	3	0.92 ± 20	2.45 ± 5	>>0	1.71 ± 5	1.51 ± 5	0.58 ± 10	–	0.37 ± 25	1.48 ± 20	0.84 ± 40	–	1.32 ± 10	1.15 ± 10	–	–
117	4	0.80 ± 25	1.85 ± 10	>0	1.32 ± 5	1.06 ± 10	0.52 ± 15	–	0.34 ± 25	1.03 ± 10	>>0	–	0.95 ± 10	0.83 ± 10	–	–
192	5	0.48 ± 20	0.99 ± 15	0.28 ± 20	0.74 ± 10	0.43 ± 10	0.30 ± 10	–	0.20 ± 30	0.54 ± 25	0.30 ± 50	–	0.57 ± 10	0.52 ± 20	–	–
242	6	0.32 ± 30	0.65 ± 20	0.28 ± 20	0.46 ± 10	0.26 ± 15	0.32 ± 10	–	0.12 ± 30	0.38 ± 20	0.19 ± 60	–	0.36 ± 15	0.30 ± 15	–	0.03 ± 40
454	7	0.11 ± 20	0.17 ± 20	0.11 ± 35	0.11 ± 20	0.06 ± 25	0.14 ± 20	–	>0	0.25 ± 20	0.13 ± 30	–	0.07 ± 25	0.14 ± 20	0.08 ± 50	–
790	8	0.06 ± 30	0.05 ± 25	0.08 ± 15	0.05 ± 30	0.02 ± 40	0.0 ± 25	–	0.06 ± 50	0.10 ± 30	0.04 ± 50	–	0.04 ± 40	0.09 ± 20	0.07 ± 50	–
1295	9	0.02 ± 50	0.02 ± 50	0.05 ± 25	0.02 ± 35	0.02 ± 50	0.03 ± 30	–	>0	0.10 ± 20	–	–	0.06 ± 35	0.07 ± 30	>0	–
240	GA 1	0.20 ± 10	0.50 ± 10		0.25 ± 30	0.12 ± 30	0.05 ± 40	–	–	0.05 ± 30	–	–	0.04 ± 60	0.08 ± 30	–	–
460	2	0.07 ± 20	0.13 ± 20	0.05 ± 20	0.06 ± 20	0.03 ± 30	>0	–	>0	0.03 ± 30	>0	–	–	0.04 ± 20	–	–
266	HA 2	11.44 ± 10	18.10 ± 7	>>0	9.65 ± 10	4.22 ± 15	3.71 ± 15	>>0	>>0	5.52 ± 10	3.60 ± 20	>>0	4.70 ± 10	6.32 ± 10	>0	0.84 ± 20
362	3	5.35 ± 7	6.81 ± 7	2.78 ± 20	4.56 ± 5	1.51 ± 15	1.76 ± 20	>>0	–	3.38 ± 10	>>0	>>0	2.18 ± 15	3.53 ± 10	>0	0.78 ± 20
459	4	4.28 ± 10	5.29 ± 10	3.00 ± 20	3.59 ± 5	0.99 ± 20	1.88 ± 20	>>0	>0	3.09 ± 10	1.40 ± 25	1.38 ± 20	1.32 ± 20	3.39 ± 10	>0	0.87 ± 20
790	5	1.07 ± 15	1.11 ± 10	1.11 ± 10	0.72 ± 10	0.24 ± 20	0.56 ± 20	0.36 ± 30	>0	1.34 ± 15	>>0	0.88 ± 20	0.18 ± 50	2.76 ± 15	>0	0.41 ± 30
983	6	0.70 ± 15	0.59 ± 15	0.83 ± 10	0.33 ± 15	0.14 ± 30	0.31 ± 25	0.18 ± 30	0.24 ± 30	1.01 ± 10	–	0.81 ± 15	0.32 ± 40	2.90 ± 15	0.30 ± 50	0.30 ± 25
987	6'	0.94 ± 20	0.57 ± 15	0.89 ± 10	0.33 ± 10	0.15 ± 30	0.31 ± 25	0.17 ± 30	0.24 ± 30	1.02 ± 10	–	0.85 ± 15	0.32 ± 30	2.90 ± 10	0.29 ± 40	0.29 ± 10
1298	7	0.32 ± 20	0.21 ± 20	0.67 ± 10	0.15 ± 20	0.07 ± 30	0.15 ± 25	0.06 ± 30	0.12 ± 30	1.44 ± 10	–	0.63 ± 10	0.25 ± 30	2.79 ± 10	0.37 ± 45	0.11 ± 30
1728.5	8	0.30 ± 30	0.19 ± 30	0.47 ± 10	0.14 ± 30	0.10 ± 30	0.06 ± 30	–	0.10 ± 30	0.96 ± 10	–	0.49 ± 10	0.15 ± 30	2.37 ± 10	0.20 ± 40	0.09 ± 50
2568.5	9	0.22 ± 20	0.11 ± 35	0.23 ± 10	0.08 ± 30	–	–	–	–	0.49 ± 10	–	0.31 ± 15	0.21 ± 35	1.87 ± 10	0.16 ± 40	–
2810	10	0.19 ± 20	0.10 ± 50	0.20 ± 20	0.07 ± 40	–	–	–	–	0.36 ± 20	–	0.26 ± 15	–	1.06 ± 10	0.10 ± 40	0.04 ± 50
359	IA 1	0.75 ± 10	1.35 ± 10	0.51 ± 25	0.78 ± 5	0.21 ± 10	0.16 ± 25	0.09 ± 20	–	0.37 ± 10	0.11 ± 25	–	0.10 ± 30	0.41 ± 10	0.10 ± 40	0.05 ± 30
460.5	2	0.52 ± 15	0.87 ± 10	0.27 ± 30	0.52 ± 5	0.0 ± 30	0.09 ± 30	>0	0.05 ± 25	0.30 ± 15	0.10 ± 20	0.05 ± 30	0.39 ± 10	0.07 ± 40	0.05 ± 30
981	3	0.10 ± 25	0.10 ± 30	0.04 ± 30	0.05 ± 25	0.03 ± 30	0.02 ± 30	–	>0	0.23 ± 15	0.02 ± 40	0.05 ± 20	–	0.33 ± 10	0.03 ± 40	0.03 ± 40
1606	4	0.06 ± 40	0.02 ± 40	0.05 ± 30	0.04 ± 40	0.03 ± 40	>0	–	–	0.17 ± 10	–	0.05 ± 35	–	0.35 ± 10	>0	>0
383	JA 1	0.47 ± 20	0.84 ± 15	0.29 ± 30	0.55 ± 10	0.16 ± 20	0.18 ± 10	0.07 ± 25	0.10 ± 30	0.34 ± 15	0.18 ± 20	–	0.21 ± 20	0.46 ± 15	0.22 ± 40	–
458	2	0.35 ± 15	0.59 ± 10	0.26 ± 30	0.43 ± 10	0.12 ± 20	0.07 ± 30	–	0.08 ± 30	0.27 ± 20	0.15 ± 30	–	0.17 ± 40	0.41 ± 15	0.14 ± 40	–
982	3	0.08 ± 25	0.08 ± 25	0.12 ± 20	0.05 ± 20	>0	0.04 ± 40	0.02 ± 30	–	0.12 ± 20	>0	0.10 ± 10	0.05 ± 30	0.35 ± 10	>0	–
1605	4	0.05 ± 20	0.04 ± 30	0.07 ± 10	0.03 ± 30	–	0.02 ± 30	–	>0	0.05 ± 30	>0	0.08 ± 20	0.04 ± 40	0.32 ± 15	–	–
96.5	KA 2	1.93 ± 30	6.27 ± 10	2.96 ± 30	3.71 ± 10	2.32 ± 15	1.35 ± 20	0.40 ± 35	0.36 ± 30	1.67 ± 15	0.50 ± 20	–	2.56 ± 5	2.28 ± 10	0.36 ± 30	0.53 ± 20
195	3	0.92 ± 10	2.32 ± 5	0.67 ± 30	1.38 ± 5	0.5 ± 15	0.56 ± 20	>0	0.16 ± 35	0.76 ± 10	>0	0.27 ± 20	0.79 ± 5	0.92 ± 5	0.28 ± 20	0.23 ± 25
262	4	0.48 ± 10	1.14 ± 5	0.37 ± 30	0.72 ± 5	0.25 ± 15	0.40 ± 10	–	0.12 ± 30	0.60 ± 10	0.20 ± 25	>0	0.48 ± 5	0.54 ± 5	0.22 ± 30	0.14 ± 25
334	5	0.38 ± 15	0.76 ± 10	0.25 ± 25	0.54 ± 10	0.17 ± 20	0.30 ± 20	–	0.13 ± 35	0.59 ± 15	0.16 ± 30	–	0.24 ± 15	0.43 ± 10	0.12 ± 40	0.11 ± 35
435	6	0.25 ± 15	0.44 ± 10	0.21 ± 15	0.27 ± 10	0.12 ± 20	0.25 ± 15	–	0.08 ± 30	0.48 ± 10	0.08 ± 25	–	0.15 ± 15	0.30 ± 15	>0	0.09 ± 30
718	7	0.08 ± 20	0.13 ± 15	0.13 ± 20	0.08 ± 15	0.03 ± 30	0.10 ± 15	–	>0	0.32 ± 10	0.04 ± 35	–	0.04 ± 25	0.23 ± 10	>0	0.07 ± 40
1031	8	0.03 ± 30	0.04 ± 15	0.07 ± 20	0.03 ± 15	0.01 ± 35	0.04 ± 20	–	0.02 ± 40	0.16 ± 15	–	–	0.02 ± 30	0.20 ± 15	–	0.03 ± 30
1558	9	0.01 ± 40	0.02 ± 30	0.05 ± 20	0.01 ± 20	–	0.03 ± 40	–	0.01 ± 50	0.12 ± 15	–	–	0.02 ± 50	0.20 ± 20	–	–
119.5	LA 1	0.66 ± 15	2.18 ± 5	>0	1.20 ± 5	0.79 ± 10	0.38 ± 15	–	0.12 ± 20	0.39 ± 20	>0	–	0.76 ± 7	0.68 ± 10	>0	–
598	2	0.05 ± 20	0.09 ± 15	0.04 ± 20	0.05 ± 10	0.02 ± 25	0.06 ± 15	–	0.01 ± 40	0.10 ± 15	0.02 ± 20	–	0.02 ± 20	0.08 ± 20	0.03 ± 40	–
337	MA 1	0.54 ± 20	0.65 ± 30	>0	0.52 ± 10	0.23 ± 20	0.39 ± 15	–	>0 0	0.57 ± 10	–	–	0.30 ± 20	0.51 ± 10	>0	–
722	2	>0	0.14 ± 20	0.10 ± 20	0.10 ± 15	>0	0.07 ± 30	0.07 ± 20	>0	0.12 ± 10	>0	–	–	0.30 ± 15	0.07 ± 40	–
1032	3	0.06 ± 20	0.06 ± 20	0.07 ± 20	0.03 ± 20	–	0.05 ± 40	–	>0	0.25 ± 15	>0	0.01 ± 35	>0	0.22 ± 20	>0	0.03 ± 30
1938	4	0.01 ± 25	0.02 ± 45	0.03 ± 30	0.02 ± 40	0.01 ± 40	>0	–	0.02 ± 25	0.10 ± 20	–	–	–	0.14 ± 25	–	0.02 ± 40
357	NA 1	1.07 ± 10	1.84 ± 10	>0	0.96 ± 5	>0	0.14 ± 30		>0	0.37 ± 15	>0	–	0.20 ± 30	0.41 ± 30	0.09 ± 5	–
20	2	0.14 ± 20	0.19 ± 10	0.12 ± 15	0.10 ± 8	>0	0.08 ± 20	–	0.05 ± 40	0.15 ± 25	0.04 ± 40	–	0.06 ± 40	0.23 ± 25	–	0.06 ± 35
1016.5	3	0.04 ± 40	0.07 ± 30	0.08 ± 25	0.03 ± 25	0.03 ± 30	0.02 ± 50	–	0.04 ± 50	0.05 ± 25	–	–	0.03 ± 50	0.10 ± 15	>0	0.04 ± 40
1538.5	4	0.02 ± 40	0.05 ± 20	>0	0.02 ± 40	–	0.02 ± 50	>0	–	0.06 ± 20	>0	–	0.02 ± 50	0.22 ± 20	0.04 ± 50	0.01 ± 50
51.5	OA 1	0.56 ± 20	0.57 ± 25	0.61 ± 30	0.36 ± 25	0.42 ± 10	0.22 ± 20	>0	>0 0	0.80 ± 10	–	–	0.82 ± 10	0.64 ± 10	>0	0.07 ± 30
69	2	0.70 ± 25	0.38 ± 25	0.46 ± 40	0.40 ± 20	0.71 ± 10	0.15 ± 20	–	>0 0	0.34 ± 15	–	0.12 ± 35	0.54 ± 10	0.41 ± 15	>0	0.07 ± 40
141	3	0.39 ± 20	0.22 ± 30	0.14 ± 40	0.1 ± 15	0.26 ± 15	0.04 ± 30	>0	>0	0.11 ± 25	>0	–	0.20 ± 20	0.19 ± 20	–	0.03 ± 35
191	4	0.14 ± 20	0.17 ± 20	0.14 ± 25	0.15 ± 20	0.20 ± 15	>0	–	0.08 ± 25	0.12 ± 20	>0	>0	0.18 ± 20	0.18 ± 20	–	0.06 ± 35
315	5	0.03 ± 30	0.04 ± 30	0.06 ± 30	0.05 ± 30	0.05 ± 30	0.05 ± 30	0.04 ± 30	>0	0.06 ± 30	>0	–	0.05 ± 25	0.05 ± 30	0.04 ± 35	–
645.5	6	0.03 ± 35	0.05 ± 40	>0	0.01 ± 35	>0	0.02 ± 55	>0	>0	0.02 ± 50	>0	–	–	0.03 ± 50	0.02 ± 50	–
197	PA 1	0.19 ± 30	0.47 ± 30	0.27 ± 40	0.32 ± 25	0.20 ± 25	0.23 ± 20	–	0.11 ± 35	0.33 ± 15	0.10 ± 25	–	0.24 ± 20	0.32 ± 20	0.13 ± 30	–
312	3	0.07 ± 25	0.16 ± 30	0.14 ± 40	0.16 ± 20	0.10 ± 30	0.18 ± 25	–	0.07 ± 40	0.30 ± 15	0.08 ± 20	–	0.12 ± 20	0.19 ± 30	0.15 ± 30	0.06 ± 30
360	4	0.07 ± 35	0.13 ± 35	0.06 ± 35	0.10 ± 30	0.06 ± 40	0.14 ± 35	–	0.07 ± 40	0.35 ± 25	0.06 ± 30	–	0.09 ± 25	0.21 ± 20	0.17 ± 30	0.08 ± 30
551	5	0.02 ± 40	0.03 ± 40	0.02 ± 40	0.02 ± 40	0.05 ± 40	0.12 ± 20	>0	0.05 ± 40	0.23 ± 15	0.04 ± 35	–	0.03 ± 45	0.12 ± 35	0.12 ± 40	0.06 ± 45
216	QA 1	0.07 ± 30	0.06 ± 30	0.05 ± 35	0.11 ± 10	>0		>0	>0	0.06 ± 20	>0	–	0.08 ± 30	0.10 ± 30	0.04 ± 40	–
360	2	0.02 ± 40	0.03 ± 30	0.02 ± 30	0.03 ± 15	–	0.04 ± 40	–	–	0.04 ± 30	>0	–	0.02 ± 30	0.05 ± 40	0.03 ± 40	–
237.5	RA 1	0.08 ± 30	0.14 ± 30	0.11 ± 20	0.14 ± 15	0.13 ± 15	0.05 ± 40	–	0.02 ± 40	0.16 ± 30	–	–	0.11 ± 15	0.15 ± 15	0.07 ± 40	0.03 ± 40
359	2	0.05 ± 30	0.04 ± 50	0.06 ± 25	0.05 ± 10	0.04 ± 20	0.03 ± 40	–	0.05 ± 30	0.10 ± 20	–	–	0.05 ± 20	0.08 ± 20	0.05 ± 50	0.02 ± 50
557	3	0.02 ± 40	0.02 ± 50	0.03 ± 40	0.03 ± 25	0.03 ± 25		–	0.03 ± 50	0.07 ± 30	–	–	0.01 ± 60	0.06 ± 25	0.02 ± 50	–
309.5	SA 1	0.04 ± 30	0.05 ± 25	0.0 ± 30	0.05 ± 25	0.05 ± 4	>0	0.02 ± 60	0.04 ± 20	0.03 ± 35	–	–	0.04 ± 25	0.06 ± 20	0.04 ± 20	0.02 ± 25
71.5	TA 1	3.48 ± 15	9.81 ± 15	>>0	7.87 ± 5	5.80 ± 5	2.59 ± 10	–	0.98 ± 10	4.55 ± 5	–	1.93 ± 20	5.61 ± 5	4.83 ± 5	>0	0.50 ± 50
93.5	2	2.73 ± 30	4.70 ± 20	>>0	6.27 ± 5	4.16 ± 7	1.86 ± 10	–	0.80 ± 30	2.77 ± 15	–	0.97 ± 30	4.09 ± 5	3.66 ± 5	>0	>0
117	3	2.48 ± 20	8.50 ± 25	>>0	4.96 ± 5	3.13 ± 10	1.59 ± 15	>0	0.60 ± 50	2.09 ± 15	–	>0	3.17 ± 10	2.69 ± 5	>0	0.70 ± 50
165	4	1.81 ± 20	6.27 ± 7	2.78 ± 25	3.67 ± 5	2.04 ± 10	1.44 ± 10	–	0.42 ± 45	1.86 ± 10	–	–	2.26 ± 10	1.99 ± 10	–	0.55 ± 20
240.5	5	1.20 ± 15	3.19 ± 10	0.85 ± 40	1.94 ± 5	0.88 ± 10	0.93 ± 10	–	0.36 ± 55	1.30 ± 10	>0	0.36 ± 25	1.03 ± 10	0.94 ± 15	0.65 ± 40	0.36 ± 15
333.5	6	0.66 ± 20	1.47 ± 10	0.56 ± 30	0.91 ± 5	0.36 ± 20	0.65 ± 15	–	>0	1.03 ± 10	>0	>0	0.50 ± 15	0.73 ± 15	>0	0.20 ± 10
424	7	0.39 ± 30	0.76 ± 15	0.36 ± 50	0.51 ± 10	0.21 ± 20	0.47 ± 20	–	>0	0.95 ± 10	>0	>0	0.28 ± 25	0.43 ± 15	>0	0.14 ± 30
578.5	8	0.22 ± 30	0.36 ± 20	0.21 ± 20	0.22 ± 25	0.12 ± 25	0.27 ± 20	–	>0	0.65 ± 15	–	>0	0.09 ± 40	0.37 ± 20	>0	0.11 ± 40
765.5	9	0.12 ± 30	0.20 ± 25	0.13 ± 20	0.09 ± 30	>0	0.18 ± 25	–	>0	0.54 ± 15	0.06 ± 40	–	0.07 ± 45	0.33 ± 20	0.15 ± 45	0.07 ± 20
1269	10	0.03 ± 35	0.05 ± 30	0.13 ± 30	0.05 ± 35	0.05 ± 50	0.05 ± 30	–	>0	0.34 ± 15	0.05 ± 30	–	0.06 ± 45	0.30 ± 20	>0	0.03 ± 50
1511	11	0.03 ± 50	0.03 ± 50	0.12 ± 15	0.02 ± 45	>0	0.02 ± 45	–	0.07 ± 40	0.26 ± 20	0.02 ± 40	–	0.02 ± 50	0.30 ± 20	0.06 ± 45	–
373	UA 1	0.66 ± 15	2.29 ± 10	0.70 ± 30	1.06 ± 5	0.57 ± 20	0.33 ± 25	–	0.18 ± 40	0.41 ± 10	–	>0	0.67 ± 5	0.61 ± 10	0.29 ± 25	–
237	2	0.47 ± 20	1.28 ± 20	0.42 ± 50	0.72 ± 10	0.32 ± 15	0.33 ± 25	–	0.11 ± 40	0.37 ± 25	>0	0.12 ± 40	0.36 ± 15	0.40 ± 25	0.18 ± 45	0.09 ± 30
312	3	0.29 ± 20	0.63 ± 15	0.1 ± 50	0.3 ± 10	0.15 ± 20	0.2 ± 30	–	0.06 ± 40	0.31 ± 25	–	0.06 ± 50	0.1 ± 20	0.26 ± 25	0.07 ± 50	0.04 ± 30
407	4	0.22 ± 15	0.38 ± 15	0.15 ± 30	0.27 ± 10	0.0 ± 20	0.14 ± 35	–	0.05 ± 60	0.27 ± 20	–	0.04 ± 50	0.10 ± 30	0.21 ± 20	>0	0.04 ± 35
576	5	0.10 ± 30	0.13 ± 30	0.06 ± 20	0.0 ± 20	0.03 ± 40	0.0 ± 30	–	0.03 ± 40	0.20 ± 25	0.04 ± 40	0.02 ± 50	0.02 ± 40	0.15 ± 30	0.04 ± 50	0.03 ± 45
238	VA 1	0.82 ± 10	2.51 ± 10	0.29 ± 35	1.11 ± 5	0.55 ± 15	0.21 ± 30	–	–	0.39 ± 30	–	>0	0.33 ± 20	0.50 ± 15	–	0.08 ± 30
335	2	0.69 ± 10	1.11 ± 10	0.22 ± 30	0.55 ± 10	0.20 ± 15	0.16 ± 30	–	0.09 ± 20	0.27 ± 10	–	–	0.17 ± 30	0.31 ± 15	–	–
413	3	0.32 ± 15	0.58 ± 10	0.14 ± 20	0.33 ± 10	0.09 ± 30	0.07 ± 30	–	0.06 ± 40	0.23 ± 15	–	–	0.06 ± 40	0.26 ± 15	>0	–
578	4	0.16 ± 20	0.28 ± 15	0.08 ± 30	0.18 ± 15	0.05 ± 40	0.07 ± 40	–	0.03 ± 50	0.26 ± 20	–	–	0.05 ± 40	0.24 ± 20	>0	0.04 ± 40
1270	5	0.02 ± 60	0.02 ± 50	0.03 ± 40	0.03 ± 35	0.02 ± 40	0.01 ± 50	–	–	0.11 ± 30	–	>0	0.02 ± 50	0.24 ± 15	–	–
1512	6	0.02 ± 50	0.01 ± 50	0.02 ± 50	>0	0.01 ± 50	>0		–	0.10 ± 30	–	0.01 ± 50	–	0.17 ± 20	–	–
243	WA 1	0.04 ± 20	0.13 ± 10	0.02 ± 50	0.09 ± 30	0.0 ± 20	0.02 ± 40	–	0.02 ± 50	0.03 ± 25	–	–	0.02 ± 50	0.02 ± 50	0.02 ± 50	–
263	KA 1	0.40 ± 10	1.37 ± 10	0.38 ± 30	0.54 ± 10	0.2 ± 20	0.09 ± 50	–	0.03 ± 40	0.14 ± 25	0.06 ± 40	>0	0.15 ± 25	0.23 ± 30	0.07 ± 45	0.04 ± 4
316	2	0.26 ± 15	0.60 ± 10	0.23 ± 30	0.34 ± 10	0.12 ± 25	0.07 ± 30	–	0.04 ± 30	0.11 ± 30	0.06 ± 50	–	0.07 ± 30	0.18 ± 15	–	–
408.5	3	0.18 ± 20	0.36 ± 10	0.10 ± 40	0.2 ± 10	0.05 ± 40	0.05 ± 60	>0	–	0.10 ± 60	0.05 ± 40	–	0.07 ± 35	0.15 ± 25	–	–
624	4	0.06 ± 30	0.11 ± 15	0.05 ± 40	0.07 ± 20	0.02 ± 40	0.03 ± 60	–	>0	0.06 ± 50	0.04 ± 30	–	0.03 ± 50	0.10 ± 20	–	–
287	TA 1	2.36 ± 10	6.10 ± 5	1.90 ± 20	3.59 ± 5	1.37 ± 15	0.82 ± 20	–	0.42 ± 30	2.34 ± 10	0.44 ± 30	–	1.68 ± 20	2.36 ± 10	–	0.46 ± 2
411	2	1.3 ± 20	2.56 ± 10	0.83 ± 30	1.52 ± 10	0.45 ± 20	0.60 ± 15	–	0.24 ± 30	1.03 ± 10	0.24 ± 30	>0	0.86 ± 20	1.61 ± 10	>0	0.27 ± 3
626	3	0.48 ± 10	0.76 ± 15	0.41 ± 20	0.54 ± 10	0.13 ± 40	0.33 ± 10	–	0.16 ± 30	1.33 ± 10	–	0.06 ± 40	0.14 ± 45	0.96 ± 10	0.16 ± 60	0.08 ± 5
767	4	0.29 ± 15	0.44 ± 15	0.33 ± 20	0.26 ± 10	0.08 ± 40	0.23 ± 20	–	0.10 ± 60	1.06 ± 15	>0	>0	–	0.90 ± 15	>0	0.09 ± 25
1271	6	0.07 ± 30	0.08 ± 60	0.14 ± 20	0.06 ± 30	0.04 ± 50	0.08 ± 35	–	0.05 ± 30	0.62 ± 15	–	0.08 ± 50	–	0.7 ± 15	>0	0.03 ±
1513	7	0.04 ± 40	–	0.17 ± 20	0.07 ± 30	–	0.07 ± 30	–	–	0.4 ± 20	–	–	0.07 ± 40	0.81 ± 20	–	0.03 ±

(a) See Table 1 or explanation of abbreviated designations. (b) Line designations energy does not necessarily represent an accurate energy calibration. The energy is rounded off to the nearest 10 kev merely as a line identification number. (c) Errors listed are in percent. • Indicates an el

38 A

TABLE 2

). in Millions of Photons Per Second Per Line for Each Sample

610	650	750	825	900	960	1040	1100	1170	1240	1370	1600	1690	2750
–	0.92 ± 10	0.88 ± 7	–	0.14 ± 20	–	–	–	–	–	–	0.25 ± 10	–	–
–	0.77 ± 6	0.62 ± 10	°0.14 ± 30	0.11 ± 20	–	–	–	–	–	–	0.25 ± 10	–	–
–	0.46 ± 10	0.47 ± 12	–	0.08 ± 40	–	–	–	–	–	–	0.25 ± 10	–	–
–	0.29 ± 10	0.28 ± 15	–	–	–	–	–	–	–	–	0.27 ± 10	–	–
–	0.21 ± 15	0.22 ± 15	–	–	–	–	–	–	–	–	0.23 ± 15	–	–
–	0.20 ± 15	0.18 ± 20	–	–	–	–	–	–	–	–	0.23 ± 15	–	–
–	0.13 ± 20	0.15 ± 20	–	–	–	–	–	–	–	–	0. 7 ± 10	–	–
–	0.10 ± 25	0.13 ± 20	–	–	–	–	–	–	–	–	0.21 ± 10	–	–
–	0.05 ± 25	0.08 ± 40	–	–	–	–	–	–	–	–	0.20 ± 10	–	–
–	0.06 ± 25	0.07 ± 30	–	–	–	–	–	–	–	–	0.15 ± 15	–	–
–	0.03 ± 50	0.06 ± 40	–	–	–	–	–	–	–	–	0.11 ± 20	–	–
–	2.57 ± 5	2.05 ± 10	–	0.58 ± 20	>0	–	–	–	–	0.73 ± 3	0.51 ± 10	–	0.59 ± 10
–	1.99 ± 7	1.48 ± 7	–	0.38 ± 20	0.34 ± 25	0.23 ± 40	–	–	–	0.38 ± 10	0.56 ± 5	–	0.22 ± 20
–	1.32 ± 10	1.15 ± 10	–	–	0.38 ± 20	0.20 ± 40	–	0.27 ± 25	–	0.18 ± 15	0.62 ± 4	–	–
–	0.98 ± 10	0.83 ± 10	–	–	0.24 ± 25	0.18 ± 30	–	0.27 ± 15	–	0.12 ± 25	0.67 ± 5	–	–
–	0.57 ± 10	0.52 ± 20	–	–	–	–	–	–	–	–	0.63 ± 10	–	–
–	0.36 ± 35	0.30 ± 35	–	0.09 ± 40	–	–	–	0.10 ± 30	–	–	0.54 ± 20	–	–
–	0.07 ± 25	0.14 ± 20	°0.08 ± 50	–	–	–	–	–	–	–	0.36 ± 15	–	–
–	0.04 ± 40	0.09 ± 20	°0.07 ± 50	–	–	–	–	–	–	–	0.17 ± 15	–	–
–	0.06 ± 35	0.07 ± 30	°>0	–	–	–	–	–	–	–	0.06 ± 30	–	–
–	0.04 ± 40	0.08 ± 30	–	–	–	–	–	–	–	–	>0	–	–
–	–	0.06 ± 28	–	–	–	–	–	>0	–	–	–	–	–
>>0	4.70 ± 10	6.32 ± 10	°>0	0.84 ± 20	–	–	–	–	–	–	6.88 ± 5	–	–
>>0	2.18 ± 15	3.53 ± 10	°>0	0.78 ± 20	–	0.66 ± 25	–	1.10 ± 20	0.59 ± 25	–	3.62 ± 10	0.59 ± 25	–
.38 ± 20	1.32 ± 20	3.39 ± 30	°>0	0.67 ± 20	–	0.50 ± 20	–	0.98 ± 20	>0	–	3.93 ± 10	>0	–
.86 ± 20	0.18 ± 50	2.76 ± 15	>0	0.21 ± 30	–	–	–	>0	0.59 ± 25	–	1.60 ± 10	0.43 ± 35	–
.27 ± 15	7.32 ± 40	2.90 ± 15	°0.30 ± 50	0.30 ± 20	–	–	–	0.62 ± 30	0.65 ± 25	–	2.36 ± 25	0.48 ± 35	–
.85 ± 15	0.32 ± 30	2.90 ± 10	°0.29 ± 40	0.29 ± 10	–	–	–	0.50 ± 30	0.50 ± 30	–	1.04 ± 15	0.50 ± 30	–
.63 ± 10	0.25 ± 30	2.79 ± 10	°0.27 ± 45	0.11 ± 30	–	–	–	0.50 ± 40	0.56 ± 30	–	0.63 ± 20	0.26 ± 60	–
.49 ± 10	0.15 ± 30	2.37 ± 10	†0.20 ± 60	0.09 ± 50	–	–	–	0.34 ± 40	0.41 ± 20	–	0.32 ± 20	0.26 ± 60	–
.31 ± 15	0.21 ± 35	1.84 ± 10	†0.16 ± 60	–	–	–	–	0.28 ± 60	0.30 ± 30	–	0.16 ± 25	0.07 ± 60	–
.26 ± 15	–	1.66 ± 10	†0.10 ± 60	0.04 ± 50	–	–	–	0.23 ± 60	0.24 ± 60	–	0.07 ± 30	0.13 ± 60	–
–	0.10 ± 30	0.61 ± 10	0.10 ± 60	0.05 ± 30	–	–	–	0.08 ± 60	0.12 ± 25	–	0.15 ± 15	–	–
–	0.05 ± 30	0.39 ± 10	0.07 ± 60	0.05 ± 30	–	–	–	0.08 ± 60	0.12 ± 25	–	0.12 ± 15	–	–
.05 ± 20	–	0.33 ± 10	0.03 ± 60	0.03 ± 60	–	–	–	0.08 ± 60	0.08 ± 30	–	0.03 ± 35	–	–
.05 ± 35	–	0.35 ± 10	>0	>0	–	–	–	0.07 ± 60	0.09 ± 30	–	>0	–	–
–	0.21 ± 20	0.46 ± 15	0.22 ± 60	–	–	–	–	0.15 ± 30	–	–	0.62 ± 10	–	–
–	0.17 ± 60	0.41 ± 15	0.14 ± 60	–	–	–	–	–	–	–	0.36 ± 10	–	–
.10 ± 10	0.05 ± 30	0.35 ± 10	>0	–	–	–	–	–	–	–	0.12 ± 15	0.07 ± 30	–
.88 ± 20	0.04 ± 60	0.32 ± 15	–	–	–	–	–	0.06 ± 60	–	–	0.06 ± 15	0.04 ± 35	–
–	2.56 ± 5	2.28 ± 10	0.36 ± 30	0.53 ± 20	–	–	–	–	–	–	0.99 ± 8	–	–
.17 ± 20	0.79 ± 5	0.92 ± 5	0.28 ± 20	0.23 ± 25	–	–	–	–	–	–	0.99 ± 3	–	–
>0	0.42 ± 5	0.54 ± 5	0.21 ± 30	0.14 ± 25	–	–	–	–	–	–	0.81 ± 5	–	–
–	0.24 ± 15	0.43 ± 10	0.12 ± 60	0.11 ± 35	–	–	–	–	–	–	0.85 ± 10	–	–
–	0.15 ± 15	0.30 ± 10	>0	0.09 ± 30	–	–	–	–	–	–	0.61 ± 10	–	–
–	0.04 ± 25	0.23 ± 10	>0	0.07 ± 60	–	–	–	–	–	–	0.34 ± 15	–	–
–	0.02 ± 30	0.20 ± 15	–	0.03 ± 30	–	–	–	–	–	–	0.15 ± 15	–	–
–	0.02 ± 50	0.20 ± 20	–	–	–	–	–	–	–	–	0.07 ± 20	–	–
–	0.76 ± 7	0.68 ± 10	>0	–	–	–	–	–	–	–	0.20 ± 15	–	–
–	0.02 ± 20	0.08 ± 20	0.03 ± 60	–	–	–	–	–	–	–	0.08 ± 20	–	–
–	0.30 ± 20	0.51 ± 10	>0	–	–	–	–	–	–	–	0.68 ± 10	–	–
–	–	0.30 ± 15	0.07 ± 60	–	–	–	–	–	–	–	0.32 ± 10	–	–
.91 ± 35	>0	0.22 ± 20	>0	0.03 ± 30	–	–	–	–	–	–	0.18 ± 15	–	–
–	–	0.14 ± 25	–	0.02 ± 60	–	–	–	–	–	–	0.0 ± 30	–	–
–	0.20 ± 30	0.41 ± 30	0.09 ± 5	–	–	–	–	–	–	–	0.68 ± 10	–	–
–	0.06 ± 60	0.23 ± 25	–	0.06 ± 35	–	–	–	–	–	–	0.27 ± 15	–	–
–	0.03 ± 50	0.30 ± 15	>0	0.05 ± 60	–	–	–	–	–	–	0.14 ± 20	–	–
–	0.02 ± 50	0.22 ± 20	0.04 ± 50	0.01 ± 50	–	–	–	–	–	–	0.04 ± 30	–	–
–	0.82 ± 10	0.64 ± 10	>0	0.07 ± 30	–	–	–	–	–	0.60 ± 25	0.13 ± 25	–	0.37 ± 20
.12 ± 35	0.54 ± 10	0.41 ± 15	>0	0.07 ± 60	–	–	0.05 ± 30	–	–	0.18 ± 25	0.14 ± 20	–	0.16 ± 30
–	0.20 ± 20	0.19 ± 20	–	0.03 ± 35	–	–	>0	–	–	0.04 ± 30	0.15 ± 25	–	–
>0	0.18 ± 20	0.18 ± 20	–	0.06 ± 35	–	–	–	–	–	–	0.19 ± 20	–	–
–	0.05 ± 25	0.05 ± 30	0.04 ± 35	–	–	–	–	–	–	–	0.11 ± 25	–	–
–	–	0.03 ± 50	0.02 ± 50	–	–	–	–	–	–	–	0.04 ± 60	–	–
–	0.24 ± 20	0.32 ± 20	0.13 ± 30	–	–	–	–	–	–	–	0.34 ± 10	–	–
–	0.12 ± 20	0.19 ± 30	0.15 ± 30	0.06 ± 30	–	–	–	–	–	–	0.41 ± 15	–	–
–	0.09 ± 25	0.21 ± 20	0.17 ± 30	0.08 ± 30	–	–	–	–	–	–	0.43 ± 15	–	–
–	0.03 ± 45	0.12 ± 35	0.12 ± 40	0.06 ± 45	–	–	–	–	–	–	0.33 ± 20	–	–
–	0.08 ± 30	0.10 ± 30	0.04 ± 60	–	–	–	–	–	–	–	0.06 ± 30	–	–
–	0.02 ± 30	0.05 ± 60	0.03 ± 60	–	–	–	–	–	–	–	0.03 ± 30	–	–
–	0.11 ± 15	0.15 ± 15	0.07 ± 60	0.03 ± 60	–	–	–	–	–	–	0.1 ± 20	–	–
–	0.05 ± 20	0.08 ± 20	0.05 ± 50	0.02 ± 50	–	–	–	–	–	–	0.16 ± 25	–	–
–	0.01 ± 60	0.06 ± 25	0.02 ± 50	–	–	–	–	–	–	–	0.09 ± 45	–	–
–	0.04 ± 25	0.06 ± 20	0.04 ± 20	0.02 ± 25	–	–	–	–	–	–	0.09 ± 30	–	–
93 ± 20	5.61 ± 5	4.83 ± 5	>0	0.50 ± 50	1.16 ± 10	–	0.46 ± 20	–	–	–	1.58 ± 10	–	0.09 ± 50
97 ± 30	4.09 ± 5	3.66 ± 5	>0	>0	0.86 ± 10	–	0.39 ± 30	–	–	–	1.60 ± 5	–	–
>0	3.17 ± 10	2.69 ± 5	>0	0.70 ± 50	0.52 ± 20	–	0.29 ± 60	–	–	–	1.72 ± 5	–	–
–	2.26 ± 10	1.99 ± 10	–	0.53 ± 20	>0	–	0.20 ± 45	–	–	–	1.81 ± 3	–	–
84 ± 25	1.03 ± 10	0.94 ± 15	0.65 ± 60	0.36 ± 15	–	–	0.14 ± 60	–	–	–	1.74 ± 5	–	–
>0	0.50 ± 15	0.73 ± 15	>0	0.20 ± 20	–	–	–	–	–	–	1.27 ± 10	–	–
>0	0.28 ± 25	0.63 ± 25	>0	0.14 ± 30	–	–	–	–	–	–	1.06 ± 15	–	–
>0	0.09 ± 60	0.37 ± 20	>0	0.11 ± 60	–	–	–	–	–	–	0.79 ± 20	–	–
–	0.07 ± 45	0.33 ± 20	0.15 ± 45	0.07 ± 20	–	–	–	–	†0.06 ± 60	–	0.52 ± 20	–	–
–	0.06 ± 45	0.30 ± 20	>0	0.03 ± 50	–	–	–	–	–	–	0.19 ± 30	–	–
–	0.02 ± 50	0.30 ± 20	0.06 ± 45	–	–	–	–	–	–	–	0.14 ± 30	–	–
°0	0.67 ± 5	0.61 ± 10	0.29 ± 25	–	0.16 ± 60	–	–	–	–	–	0.27 ± 20	–	–
12 ± 60	0.36 ± 15	0.60 ± 15	0.16 ± 45	0.09 ± 30	–	–	–	–	–	–	0.28 ± 20	–	–
36 ± 50	0.19 ± 20	0.26 ± 25	0.07 ± 50	0.08 ± 30	–	–	–	–	–	–	0.24 ± 15	–	–
24 ± 50	0.10 ± 30	0.21 ± 20	>0	0.06 ± 35	–	–	–	–	–	–	0.21 ± 15	–	–
22 ± 50	0.02 ± 60	0.15 ± 30	0.06 ± 50	0.03 ± 45	–	–	–	–	–	–	0.16 ± 25	–	–
>0	0.33 ± 20	0.50 ± 15	–	0.08 ± 30	–	–	–	–	–	–	0.21 ± 10	–	–
–	0.17 ± 30	0.31 ± 15	–	–	–	–	–	–	–	–	0.17 ± 15	–	–
–	0.06 ± 60	0.26 ± 15	>0	–	–	–	–	–	–	–	0.14 ± 20	–	–
–	0.05 ± 60	0.24 ± 20	>0	0.06 ± 60	–	–	–	–	–	–	0.08 ± 25	–	–
>0	0.02 ± 50	0.24 ± 15	–	–	–	–	–	–	–	–	>0	–	–
31 ± 50	–	0.17 ± 20	–	–	–	–	–	–	–	–	>0	–	–
–	0.02 ± 50	0.02 ± 50	0.02 ± 50	–	–	–	–	–	–	–	0.03 ± 25	–	–
>0	0.15 ± 25	0.23 ± 20	0.07 ± 45	0.04 ± 45	–	–	–	–	–	–	0.18 ± 20	–	–
–	0.05 ± 50	0.18 ± 15	–	–	–	–	–	–	–	–	0.16 ± 20	–	–
–	0.07 ± 35	0.15 ± 15	–	–	–	–	–	–	–	–	0.14 ± 25	–	–
–	0.03 ± 50	0.10 ± 20	–	–	–	–	–	–	–	–	0.07 ± 30	–	–
–	1.68 ± 20	2.36 ± 10	–	0.46 ± 25	0.25 ± 30	–	†0.27 ± 15	–	–	–	2.51 ± 5	–	–
>0	0.66 ± 20	1.61 ± 10	>0	0.27 ± 30	–	–	†0.18 ± 25	–	–	–	1.70 ± 5	–	–
26 ± 60	0.12 ± 45	0.96 ± 10	†0.16 ± 60	0.08 ± 50	–	–	†0.08 ± 30	–	†0.16 ± 20	–	1.06 ± 10	–	–
>0	>0	0.90 ± 15	>0	0.09 ± 25	–	–	†0.08 ± 50	–	–	–	0.86 ± 20	–	–
38 ± 50	–	0.73 ± 15	>0	0.05 ± 40	–	–	†0.06 ± 50	–	†0.08 ± 50	–	0.26 ± 20	–	–
–	0.07 ± 60	0.81 ± 20	–	0.03 ± 40	–	–	†0.04 ± 50	–	†0.04 ± 60	–	0.16 ± 25	–	–

(c) Errors listed are in percent. ° Indicates an energy shift 20-30 mev below line designation. † Indicates an energy shift 20-30 mev above line designation.

TABLE 3

Absolute Photon Intensities (High Gain), in Millions of Photons Per Second Per Line From Each Recording

Time After Shot (hr)	Sample and Recording[a]	Line Designation (kev)[b] 16 – 20	30 – 35	60	105	140	220	280
51	AB 1	1.08 ± 40[c]	0.24 ± 40	0.54 ± 25	4.44 ± 10	0.87 ± 15	1.43 ± 15	1.02 ± 15
75	2	1.08 ± 40	0.24 ± 50	0.64 ± 20	3.87 ± 10	0.64 ± 15	1.14 ± 15	0.67 ± 20
99	3	0.85 ± 40	>0	0.47 ± 20	2.78 ± 15	0.48 ± 15	0.89 ± 15	0.66 ± 25
166	4	0.35 ± 50	0.18 ± 50	0.41 ± 20	1.40 ± 15	0.33 ± 20	0.52 ± 20	0.26 ± 30
191.5	5	0.18 ± 50	>0	0.24 ± 20	1.05 ± 20	0.16 ± 20	0.35 ± 25	0.10 ± 40
215	6	0.15 ± 50	>0	0.18 ± 25	0.69 ± 25	0.11 ± 30	0.23 ± 30	0.05 ± 45
263	8	>0	-	0.17 ± 30	0.50 ± 25	0.07 ± 40	0.18 ± 30	-
335	9	>0	-	0.17 ± 40	0.32 ± 30	0.06 ± 45	0.11 ± 40	-
406	10	-	-	0.10 ± 40	0.17 ± 35	>0	0.09 ± 40	-
53	BB 1	1.70 ± 50	0.85 ± 50	1.33 ± 50	4.27 ± 10	0.72 ± 20	1.63 ± 25	2.09 ± 20
70	2	1.40 ± 50	0.85 ± 50	1.18 ± 30	3.63 ± 15	0.72 ± 30	1.54 ± 25	1.77 ± 20
96	3	1.00 ± 25	0.50 ± 50	1.12 ± 30	2.53 ± 15	0.48 ± 30	1.06 ± 25	1.02 ± 20
118	4	0.77 ± 30	0.36 ± 50	0.60 ± 30	2.09 ± 20	0.30 ± 30	0.72 ± 30	0.55 ± 30
193	5	0.54 ± 35	>0	0.59 ± 35	1.21 ± 20	0.30 ± 30	0.52 ± 30	0.26 ± 35
244	6	0.34 ± 40	-	0.41 ± 35	0.74 ± 20	0.14 ± 35	0.30 ± 30	>0
454.5	7	0.17 ± 35	-	0.17 ± 40	0.26 ± 25	0.12 ± 40	0.13 ± 45	-
795	8	0.05 ± 30	-	-	0.04 ± 35	0.07 ± 35	-	-
1296	9	-	0.03 ± ?	-	-	0.04 ± 40	-	-
242	GB 1	0.05 ± 40	-	0.19 ± 30	0.56 ± 10	0.11 ± 40	0.11 ± 50	-
244.5	HB 1[d]	2.10 ± 25	-	7.00 ± 15	20.59 ± 10	3.85 ± 30	7.31 ± 10	1.76 ± 40
360	3[d]	1.20 ± 30	-	3.26 ± 20	7.58 ± 20	1.11 ± 30	2.85 ± 20	-
863	5[e]	0.67 ± 30	-	1.21 ± 30	1.33 ± 25	1.05 ± 30	0.60 ± 25	-
1060	6[d]	>0	-	0.72 ± 30	0.51 ± 30	0.74 ± 25	0.22 ± 35	-
1299	7	0.23 ± 30	-	0.61 ± 30	0.34 ± 40	0.59 ± 25	>0	-
1730	8	0.12 ± 50	-	0.45 ± 30	0.12 ± 50	0.43 ± 30	>0	-
2570	9	0.09 ± 50	-	0.32 ± 40	0.08 ± 50	0.23 ± 40	-	-
360	IB 1	0.31 ± 40	0.17 ± 35	1.02 ± 10	1.64 ± 20	0.30 ± 25	0.74 ± 15	-
384	JB 1	0.25 ± 50	0.16 ± 30	0.59 ± 15	0.94 ± 15	0.22 ± 30	0.34 ± 30	-
458.5	2	0.12 ± 50	0.06 ± 40	0.50 ± 20	0.73 ± 20	>0	0.41 ± 40	-
75	KB 1	1.68 ± 50	0.75 ± ?	1.44 ± 40	7.79 ± 10	1.84 ± 20	2.57 ± 15	1.77 ± 30
97	2	1.55 ± 50	0.75 ± ?	1.23 ± 25	6.95 ± 10	1.55 ± 25	2.17 ± 20	1.01 ± 30
196	3	0.78 ± 40	0.27 ± ?	0.93 ± 20	2.79 ± 15	0.63 ± 25	0.95 ± 20	0.34 ± 30
262	4	0.39 ± ?	—	0.57 ± 30	1.38 ± 20	0.31 ± 40	0.51 ± 30	-
335	5	0.27 ± 50	0.09 ± ?	0.31 ± 30	0.63 ± 20	0.14 ± 40	0.23 ± 30	-
436	6	0.07 ± 50	0.03 ± ?	0.10 ± 30	0.20 ± 20	0.04 ± 25	0.09 ± 25	-
719	7	0.05 ± ?	-	0.04 ± ?	0.07 ± ?	0.05 ± ?	0.03 ± ?	-
96	LB 1	0.46 ± 35	0.28 ± 50	0.68 ± 20	2.70 ± 10	0.63 ± 40	0.84 ± 30	0.42 ± 40
338	MB 1	0.19 ± 30	-	0.39 ± 40	1.05 ± 10	0.19 ± 30	0.36 ± 20	-
723	2	0.08 ± 40	0.03 ± 50	0.11 ± 30	0.16 ± 20	0.11 ± 30	0.07 ± 40	-
358	NB 1	0.32 ± 45	0.18 ± 50	0.61 ± 20	1.07 ± 15	0.26 ± 40	0.44 ± 30	0.05 ± 50
720	2	0.07 ± 50	0.08 ± 40	0.16 ± 25	0.17 ± 20	0.14 ± 40	0.10 ± 40	-
52	OB 1	0.35 ± 30	0.17 ± 50	0.61 ± 25	0.56 ± 20	0.31 ± 30	0.30 ± 40	0.70 ± 25
70	2	0.26 ± 40	0.13 ± 50	0.46 ± 30	0.34 ± 30	0.26 ± 30	0.18 ± 40	0.44 ± 30
147	3	0.11 ± 50	0.06 ± 50	0.16 ± 40	0.16 ± 35	0.14 ± 40	0.06 ± 50	0.14 ± 40
192	4	0.08 ± 50	0.05 ± 50	0.15 ± 50	0.15 ± 50	0.09 ± 50	>0	0.10 ± 50
214	PB 2	0.19 ± 35	0.07 ± 50	0.16 ± 30	0.58 ± 25	0.20 ± 30	0.23 ± 35	0.07 ± 50
218	QB 1	0.04 ± 60	0.09 ± 30	0.08 ± 40	0.13 ± 30	0.07 ± 40	0.09 ± 40	0.05 ± 50
238	RB 1	0.07 ± 50	0.06 ± 50	0.10 ± 40	0.16 ± 35	0.09 ± 40	0.09 ± 40	0.14 ± 30
74	TB 1	2.24 ± 25	-	1.66 ± 30	15.59 ± 10	2.75 ± 35	6.27 ± 15	4.41 ± 20
94	2	2.10 ± 20	-	1.63 ± 20	13.24 ± 10	2.80 ± 30	4.73 ± 15	3.54 ± 20
118	3	1.77 ± 20	-	1.36 ± 20	10.41 ± 10	2.00 ± 30	3.99 ± 15	2.55 ± 25
167	4	1.61 ± 20	-	1.39 ± 25	7.14 ± 10	1.55 ± 35	3.02 ± 15	1.68 ± 30
242	5	0.88 ± 20	-	0.97 ± 25	3.47 ± 15	0.80 ± 25	1.37 ± 15	0.70 ± 50
335	6	0.65 ± 20	-	0.70 ± 20	1.85 ± 15	0.52 ± 30	0.71 ± 20	0.25 ± 50
431	7	0.42 ± 25	-	0.48 ± 25	0.95 ± 15	0.31 ± 25	0.47 ± 25	-
580	8	0.21 ± 30	-	0.25 ± 25	0.45 ± 20	0.22 ± 25	0.21 ± 35	-
767	9	0.17 ± 30	>0	0.17 ± 30	0.26 ± 25	0.25 ± 40	0.09 ± 40	-
239	UB 2	0.44 ± 25	-	0.46 ± 15	1.48 ± 15	0.40 ± 20	0.52 ± 20	0.13 ± 40
314	3	0.29 ± 30	-	0.38 ± 20	0.77 ± 15	0.14 ± 25	0.29 ± 30	-
408	4	0.19 ± 30	-	0.29 ± 25	0.55 ± 25	0.11 ± 30	0.17 ± 30	-
239.5	VB 1	0.52 ± 30	0.16 ± 40	0.80 ± 25	2.29 ± 20	0.28 ± 30	0.79 ± 20	0.34 ± 30
336	2	0.26 ± 30	0.09 ± 40	0.45 ± 25	1.07 ± 15	0.09 ± 40	0.30 ± 25	-
432	3	0.17 ± 35	0.07 ± 50	0.32 ± 20	0.82 ± 15	0.08 ± 50	0.43 ± 40	-
263	XB 1	0.21 ± 30	-	0.50 ± 30	1.24 ± 15	0.42 ± 20	0.41 ± 20	0.16 ± 40
316.5	2	0.13 ± 30	-	0.31 ± 30	0.74 ± 10	0.14 ± 30	0.30 ± 25	-
410	3	0.13 ± 40	-	0.28 ± 40	0.48 ± 25	0.11 ± 40	0.17 ± 40	-
287	YB 1	1.09 ± 20	-	1.98 ± 20	6.70 ± 10	1.39 ± 25	2.45 ± 20	0.52 ± 60
314	2	0.97 ± 20	0.58 ± 50	1.81 ± 20	5.17 ± 10	1.11 ± 25	1.71 ± 20	0.30 ± 40
412	3	0.73 ± 30	0.52 ± 30	1.39 ± 25	3.07 ± 15	0.72 ± 20	1.20 ± 15	-
626	4	0.32 ± 40	0.28 ± 40	0.55 ± 25	0.96 ± 20	0.43 ± 25	0.39 ± 20	-
768	5	0.20 ± 40	0.15 ± 50	0.33 ± 25	0.56 ± 25	0.31 ± 25	0.17 ± 30	-

(a) See Table 1 for explanation of abbreviated designations.
(b) Line designation energy does not necessarily represent an accurate energy calibration. The energy is rounded off to the nearest 10 kev merely as a line identification number.
(c) Errors listed are in percent.
(d) >0 at 165 kev.
(e) 0.40 ± 50 percent at 165 kev.

[redacted]

DISTRIBUTION

Copies

NAVY

1-9	Chief, Bureau of Ships (Code 348)
10	Chief, Bureau of Medicine and Surgery
11	Chief, Bureau of Aeronautics (Code AE40)
12	Chief, Bureau of Supplies and Accounts (Code W)
13-14	Chief, Bureau of Yards and Docks (D-440)
15	Chief of Naval Operations (Op-36)
16	Chief of Naval Operations (Op-361)
17	Commander, New York Naval Shipyard (Material Lab.)
18	Director, Naval Research Laboratory (Code 2021)
19	Director, Naval Research Laboratory (Code 1501)
20	CO, Naval Unit, Army Chemical Center
21	CO, U. S. Naval Civil Engineering (Res. and Eval. Lab.)
22	U. S. Naval School (CEC Officers)
23	Commander, Naval Air Material Center, Philadelphia
24	Commander, Naval Air Development and Material Center
25	CO, Naval Schools Command, Treasure Island
26	CO, Naval Damage Control Training Center, Philadelphia
27	U. S. Naval Postgraduate School, Monterey
28	CO, Fleet Training Center, Norfolk
29-30	CO, Fleet Training Center, San Diego
31	Commandant, Twelfth Naval District
32	Office of Patent Counsel, Mare Island
33	Commander Air Force, Atlantic Fleet (Code 16F)
34	CO, Fleet Airborne Electronics Training Unit Atlantic
35	Commandant, U. S. Marine Corps
36	Commandant, Marine Corps Schools, Quantico (Library)
37	Commandant, Marine Corps Schools, Quantico (Development Center)

ARMY

38	Chief of Engineers (ENGEB, Dhein)
39	Chief of Engineers (ENGNB)
40-41	Chief of Research and Development (Atomic Division)
42	Chief of Transportation (TC Technical Committee)
43	Chief of Ordnance (ORDTB)
44	Chief Chemical Officer

[redacted]

[redacted]

45	Deputy Chief of Staff for Military Operations
46	CG, Chemical Corps Research and Development Command
47	CO, Hq., Chemical Corps Materiel Command
48	President, Chemical Corps Board
49	CO, Chemical Corps Training Command (Library)
50	CO, Chemical Corps Field Requirements Agency
51-52	CO, Chemical Warfare Laboratories
53	Office of Chief Signal Officer (SIGRD-8B)
54	Director, Walter Reed Army Medical Center
55	CG, Continental Army Command, Fort Monroe (ATDEV-1)
56	CG, Quartermaster Res. and Dev. Command
57	Director, Operations Research Office (Librarian)
58	CO, Dugway Proving Ground
59	Director, Evans Signal Laboratory (Nucleonics Section)
60	CG, Engineer Res. and Dev. Laboratory (Library)
61	CO, Transportation Res. and Dev. Command, Fort Eustis
62	Commandant, Army Aviation School, Fort Rucker
63	President, Board No. 6, CONARC, Fort Rucker
64	NLO, CONARC, Fort Monroe
65	Director, Special Weapons Development, Fort Bliss
66	CO, Ordnance Materials Research Office, Watertown

AIR FORCE

67	Directorate of Intelligence (AFOIN-3B)
68	Assistant Secretary of the Air Force
69	Commander, Air Materiel Command (MCMTM)
70	Commander, Wright Air Development Center (WCRTY)
71	Commander, Wright Air Development Center (WCRTH-1)
72-74	Commander, Wright Air Development Center (WCOSI-3)
75	Commander, Air Res. and Dev. Command (RDTDA)
76	Director, USAF Project RAND (WEAPD)
77	Commander, Air Technical Intelligence Center (AFOIN-ATIAW)
78	Commandant, School of Aviation Medicine, Randolph AFB
79	CG, Strategic Air Command, Offutt AFB (IGABD)
80	CG, Strategic Air Command (Operations Analysis Office)
81	Commander, Special Weapons Center, Kirtland AFB
82	Director, Air University Library, Maxwell AFB
83	Commander, Technical Training Wing, 3415th TTG
84	CG, Cambridge Research Center (CRHTM)
85	CO, Air Weather Service - MATS, Langley AFB
86	AFOAT - Headquarters

OTHER DOD ACTIVITIES

87	Chief, Armed Forces Special Weapons Project
88	AFSWP, SWTG, Sandia Base (Library)
89-91	AFSWP, Hq., Field Command, Sandia Base
92	Assistant Secretary of Defense (Res. and Dev.)

[redacted]

[redacted]

AEC ACTIVITIES AND OTHERS

(For addressees below, transmission is made via specific transfer-accountability stations designated by the AEC.)

93	Argonne National Laboratory
94-96	Atomic Energy Commission, Washington
97-98	Bettis Plant (WAPD)
99-100	Boeing Airplane Company, Seattle
101	Brookhaven National Laboratory
102-103	duPont Company, Aiken
104-105	General Electric Company (ANPD)
106-108	General Electric Company, Richland
109	Hanford Operations Office
110-111	Knolls Atomic Power Laboratory
112-113	Los Alamos Scientific Laboratory
114	Lovelace Foundation
115	National Lead Company of Ohio
116	New York Operations Office
117-118	Phillips Petroleum Company (NRTS)
119	Public Health Service
120	San Francisco Operations Office
121	Sandia Corporation
122	Sandia Corporation, Livermore
123-124	Union Carbide Nuclear Company (K-25 Plant)
125-127	Union Carbide Nuclear Company (ORNL)
128	UCLA Medical Research Laboratory
129-130	University of California Radiation Laboratory, Berkeley
131-132	University of California Radiation Laboratory, Livermore
133	University of Rochester
134-148	Technical Information Service Extension, Oak Ridge

USNRDL

149-175	USNRDL, Technical Information Division

DATE ISSUED: 19 July 1957

[redacted]